TCRP

REPORT 71, Volume 2

TRANSIT COOPERATIVE RESEARCH PROGRAM

Sponsored by the Federal Transit Administration

Transit Switch Design Analysis (Phase I)

TRANSPORTATION RESEARCH BOARD
OF THE NATIONAL ACADEMIES

TRANSIT COOPERATIVE RESEARCH PROGRAM

TCRP REPORT 71, Volume 2

Transit Switch Design Analysis (Phase 1)

SATYA P. SINGH
DAVID D. DAVIS
and
SEMIH KALAY
Transportation Technology Center, Inc.
Pueblo, CO

SUBJECT AREAS
Public Transit • Rail

Research Sponsored by the Federal Transit Administration in Cooperation with the Transit Development Corporation

TRANSPORTATION RESEARCH BOARD

WASHINGTON, D.C.
2003
www.TRB.org

TRANSIT COOPERATIVE RESEARCH PROGRAM

The nation's growth and the need to meet mobility, environmental, and energy objectives place demands on public transit systems. Current systems, some of which are old and in need of upgrading, must expand service area, increase service frequency, and improve efficiency to serve these demands. Research is necessary to solve operating problems, to adapt appropriate new technologies from other industries, and to introduce innovations into the transit industry. The Transit Cooperative Research Program (TCRP) serves as one of the principal means by which the transit industry can develop innovative near-term solutions to meet demands placed on it.

The need for TCRP was originally identified in *TRB Special Report 213—Research for Public Transit: New Directions*, published in 1987 and based on a study sponsored by the Urban Mass Transportation Administration—now the Federal Transit Administration (FTA). A report by the American Public Transportation Association (APTA), *Transportation 2000*, also recognized the need for local, problem-solving research. TCRP, modeled after the longstanding and successful National Cooperative Highway Research Program, undertakes research and other technical activities in response to the needs of transit service providers. The scope of TCRP includes a variety of transit research fields including planning, service configuration, equipment, facilities, operations, human resources, maintenance, policy, and administrative practices.

TCRP was established under FTA sponsorship in July 1992. Proposed by the U.S. Department of Transportation, TCRP was authorized as part of the Intermodal Surface Transportation Efficiency Act of 1991 (ISTEA). On May 13, 1992, a memorandum agreement outlining TCRP operating procedures was executed by the three cooperating organizations: FTA; the National Academies, acting through the Transportation Research Board (TRB); and the Transit Development Corporation, Inc. (TDC), a nonprofit educational and research organization established by APTA. TDC is responsible for forming the independent governing board, designated as the TCRP Oversight and Project Selection (TOPS) Committee.

Research problem statements for TCRP are solicited periodically but may be submitted to TRB by anyone at any time. It is the responsibility of the TOPS Committee to formulate the research program by identifying the highest priority projects. As part of the evaluation, the TOPS Committee defines funding levels and expected products.

Once selected, each project is assigned to an expert panel, appointed by the Transportation Research Board. The panels prepare project statements (requests for proposals), select contractors, and provide technical guidance and counsel throughout the life of the project. The process for developing research problem statements and selecting research agencies has been used by TRB in managing cooperative research programs since 1962. As in other TRB activities, TCRP project panels serve voluntarily without compensation.

Because research cannot have the desired impact if products fail to reach the intended audience, special emphasis is placed on disseminating TCRP results to the intended end users of the research: transit agencies, service providers, and suppliers. TRB provides a series of research reports, syntheses of transit practice, and other supporting material developed by TCRP research. APTA will arrange for workshops, training aids, field visits, and other activities to ensure that results are implemented by urban and rural transit industry practitioners.

The TCRP provides a forum where transit agencies can cooperatively address common operational problems. The TCRP results support and complement other ongoing transit research and training programs.

TCRP REPORT 71, Volume 2

Project D-07(2) FY'99
ISSN 1073-4872
ISBN 0-309-06701-3
Library of Congress Control Number 2001135523

Price $18.00

NOTICE

The project that is the subject of this report was a part of the Transit Cooperative Research Program conducted by the Transportation Research Board with the approval of the Governing Board of the National Research Council. Such approval reflects the Governing Board's judgment that the project concerned is appropriate with respect to both the purposes and resources of the National Research Council.

The members of the technical advisory panel selected to monitor this project and to review this report were chosen for recognized scholarly competence and with due consideration for the balance of disciplines appropriate to the project. The opinions and conclusions expressed or implied are those of the research agency that performed the research, and while they have been accepted as appropriate by the technical panel, they are not necessarily those of the Transportation Research Board, the National Research Council, the Transit Development Corporation, or the Federal Transit Administration of the U.S. Department of Transportation.

Each report is reviewed and accepted for publication by the technical panel according to procedures established and monitored by the Transportation Research Board Executive Committee and the Governing Board of the National Research Council.

Special Notice

The Transportation Research Board, the National Research Council, the Transit Development Corporation, and the Federal Transit Administration (sponsor of the Transit Cooperative Research Program) do not endorse products or manufacturers. Trade or manufacturers' names appear herein solely because they are considered essential to the clarity and completeness of the project reporting.

Published reports of the

TRANSIT COOPERATIVE RESEARCH PROGRAM

are available from:

Transportation Research Board
Business Office
500 Fifth Street, NW
Washington, DC 20001

and can be ordered through the Internet at
http://www.national-academies.org/trb/bookstore

Printed in the United States of America

THE NATIONAL ACADEMIES

Advisers to the Nation on Science, Engineering, and Medicine

The **National Academy of Sciences** is a private, nonprofit, self-perpetuating society of distinguished scholars engaged in scientific and engineering research, dedicated to the furtherance of science and technology and to their use for the general welfare. On the authority of the charter granted to it by the Congress in 1863, the Academy has a mandate that requires it to advise the federal government on scientific and technical matters. Dr. Bruce M. Alberts is president of the National Academy of Sciences.

The **National Academy of Engineering** was established in 1964, under the charter of the National Academy of Sciences, as a parallel organization of outstanding engineers. It is autonomous in its administration and in the selection of its members, sharing with the National Academy of Sciences the responsibility for advising the federal government. The National Academy of Engineering also sponsors engineering programs aimed at meeting national needs, encourages education and research, and recognizes the superior achievements of engineers. Dr. William A. Wulf is president of the National Academy of Engineering.

The **Institute of Medicine** was established in 1970 by the National Academy of Sciences to secure the services of eminent members of appropriate professions in the examination of policy matters pertaining to the health of the public. The Institute acts under the responsibility given to the National Academy of Sciences by its congressional charter to be an adviser to the federal government and, on its own initiative, to identify issues of medical care, research, and education. Dr. Harvey V. Fineberg is president of the Institute of Medicine.

The **National Research Council** was organized by the National Academy of Sciences in 1916 to associate the broad community of science and technology with the Academy's purposes of furthering knowledge and advising the federal government. Functioning in accordance with general policies determined by the Academy, the Council has become the principal operating agency of both the National Academy of Sciences and the National Academy of Engineering in providing services to the government, the public, and the scientific and engineering communities. The Council is administered jointly by both the Academies and the Institute of Medicine. Dr. Bruce M. Alberts and Dr. William A. Wulf are chair and vice chair, respectively, of the National Research Council.

The **Transportation Research Board** is a division of the National Research Council, which serves the National Academy of Sciences and the National Academy of Engineering. The Board's mission is to promote innovation and progress in transportation by stimulating and conducting research, facilitating the dissemination of information, and encouraging the implementation of research results. The Board's varied activities annually engage more than 4,000 engineers, scientists, and other transportation researchers and practitioners from the public and private sectors and academia, all of whom contribute their expertise in the public interest. The program is supported by state transportation departments, federal agencies including the component administrations of the U.S. Department of Transportation, and other organizations and individuals interested in the development of transportation. **www.TRB.org**

www.national-academies.org

COOPERATIVE RESEARCH PROGRAMS STAFF

ROBERT J. REILLY, *Director, Cooperative Research Programs*
CHRISTOPHER W. JENKS, *TCRP Manager*
EILEEN P. DELANEY, *Managing Editor*
HILARY FREER, *Associate Editor II*

PROJECT PANEL D-07(2)
Field of Engineering of Fixed Facilities

ANTHONY BOHARA, *Southeastern Pennsylvania Transportation Authority* (Chair)
STELIAN CANJEA, *New Jersey Transit Corporation*
LANCE G. COOPER, *Olney, MD*
EARLE M. HUGHES, *Gannett Fleming Transit & Rail Systems, Audubon, PA*
JAMES NELSON, *Wilson, Ihrig & Associates, Inc., Oakland, CA*
JOSEPH A. ORIOLO, *Massachusetts Bay Transportation Authority*
FREDERICK E. SMITH, *Metropolitan Transportation Authority—New York City Transit*
CHARLES L. STANFORD, *Houston, TX*
JEFFREY G. MORA, *FTA Liaison Representative*
LOUIS F. SANDERS, *APTA Liaison Representative*
GUNARS SPONS, *FRA Liaison Representative*
ELAINE KING, *TRB Liaison Representative*

FOREWORD

By Christopher W. Jenks
Staff Officer
Transportation Research Board

This report presents the results of a research task carried out under TCRP Project D-7, *Joint Rail Transit-Related Research with the Association of American Railroads/Transportation Technology Center, Inc., Transit Switch Design Analysis (Phase I).* Under this task, a new switch design concept for transit was developed. A prototype of the switch will be produced and tested in Phase II of the effort. This report should be of interest to engineers responsible for design, construction, maintenance, and operation of rail transit systems.

Over the years, a number of track-related research problem statements have been submitted for consideration in the TCRP project-selection process. In many instances, the research requested has been similar to research currently being performed for the Federal Railroad Administration (FRA) and the freight railroads by the Association of American Railroads' (AAR) Transportation Technology Center, Inc. (TTCI) in Pueblo, Colorado. Transit track, signal, and rail vehicle experts reviewed the research being conducted by TTCI. Based on this effort, several research topics were identified where TCRP funding could be used to take advantage of research currently being performed at the TTCI for the benefit of the transit industry. A final report on one of these efforts is presented in this publication.

Transit Switch Design Analysis (Phase I)

Transit switch designs in the early 1900s were quite sophisticated by today's standards. These switches gave excellent service for many years, often outliving the lower cost but simpler replacement designs that followed. Many of the earlier designs became obsolete because most were unique to a particular transit system, and in some cases, casting patterns are no longer available.

At a number of transit systems, it has been observed that often the best-performing switches on their systems were the oldest switches. The original switches often had service lives of 50 years or more and often outlive replacement switches by 100 to 1,000%.

In this project, TTCI modeled the performance of trains operating over an older, tangential design spiraled geometry Number 8 turnout, an AREMA Number 8 lateral turnout with a curved switch design, and several variations of these two designs. The study was designed to determine the switch characteristics that contribute to the good performance and long life of the older switches. Based on this evaluation, a switch design encompassing these characteristics was developed. A prototype of this design will be produced and field tested in Phase II of the project.

CONTENTS

TRANSIT SWITCH DESIGN ANALYSIS (PHASE I)

SUMMARY

Transportation Technology Center, Inc. (TTCI), a wholly owned subsidiary of the Association of American Railroads (AAR), modeled the performance of Southeastern Pennsylvania Transportation Authority (SEPTA) B-IV cars operating over a SEPTA tangential design spiraled geometry Number 8 lateral turnout, an American Railway Engineering Maintenance-of-Way Association (AREMA) Number 8 lateral turnout with a 13-ft curved switch design, and several variations of these two designs. The study was designed to determine which switch design features contribute to the good performance and long service life of the SEPTA switches. These design elements will be applied to current switch design to develop a low-cost, high-performance switch for future use.

No discussion of switch geometry is complete without the rest of the turnout. The selection of switch geometry affects the turnout closure curve alignment. The relative lengths of the SEPTA car versus the switch and turnout make inclusion of the entire turnout essential to the study. The switch is 13 ft long with the lead length of the number 8 turnout being 57 ft. The B-IV car is 68 ft long with the truck spacing producing a 48-ft wheelbase. Thus, when the trailing truck of the car is moving through the switch, the lead truck is moving through the frog. Thus, the track modeled included the entire turnout with track beyond the frog being tangent at the frog angle. To reflect the actual analysis done, the term “turnout” is used in the report, even though the focus of the study is clearly on the switch design. In most of the scenarios modeled, the switch produced the maximum forces or accelerations. However, in some operating scenarios, the turnout closure curve alignment may generate the maximum forces or accelerations.

The as-built SEPTA tangential design spiraled geometry Number 8 lateral turnout performs well in comparison with the per-plan AREMA Number 8 secant, circular geometry switch turnout. In its intended service of 5- to 15-mph operation, the switch is superior to the AREMA switch in minimizing loads and accelerations. However, the SEPTA switch turnout does show higher than desired accelerations under B-IV car operations. This may cause ride quality concerns at higher speeds.

Parametric studies of some design features were conducted to determine their effects on switch performance. Tangential switch entry is essential to the good performance of the SEPTA switch. Elimination of a kink angle and its resultant abrupt spike in dynamic

loading produce a smooth ride and more even switch wear. The spiral switch entry and exit curves are effective at smoothing the ride through the switch, minimizing jerk by evening out the change in accelerations. However, the very small radius of closure curve may adversely affect ride quality for certain types of equipment (i.e., longer cars) or service (higher speeds).

The advantages of the SEPTA switch turnout are not fully realized because of the longer length of the B-IV cars. The extremely short radius closure curves of the turnout cause the cars to "stringline," creating relatively high lateral forces. These forces increase rapidly with speed. The AREMA designs, with their larger radius closure curves, better accommodate the longer cars at higher speeds.

The use of Austenitic Manganese Steel (AMS) castings for the switch points in the SEPTA switch produces a tough, durable switch point. When introduced, the AMS point was vastly superior to rail steels of the time. However, modern rail steels perform as well as AMS in curve wear. The layout of current switches, with good geometry and guardrails, make the advantages of AMS almost redundant. The high cost of fabricating AMS switch points makes it an uneconomic choice for modern switches.

The housed switch point is a feature that provides benefits for switches with significant diverging traffic. The switch point is thickened to make it more robust and diminish the risk of split switch derailments. The stock rail is diminished to accomplish this, which may result in a foreshortened life for this component. A housing would help to eliminate the sharp dynamic loading and localized wear at the point of switch on AREMA switches seen in the field, as well as those seen in NUCARS™ simulations done for this study. The running surface discontinuity at the point of switch seen at the gage face is especially important if guardrails are not used in the switch.

Guardrails in the switch are needed for safety reasons. The guardrails ensure that a safe operation is maintained as the switch wears and deforms. The guardrail and back of wheel flange contact are nearly vertical, even on worn components. Thus, wheel climb is less likely than with worn wheel flange/switch point contact. As for switch performance, the dynamic loads in the switch are little changed. Switch point life is improved by transferring wear from switch point to guard rail.

Use of guardrails in front of the switch protects the switch points from impacts. The good switch geometry and housed point design of the SEPTA switch diminishes the effectiveness of the guardrails.

Separating the point of switch from the point of curvature (or point of spiral in the case of the SEPTA switch), where the point of curvature comes first, is good for relatively low-speed mainline operations. The mainline trains have to negotiate a small curve as a penalty for making the diverging route curve somewhat larger. This design is a compromise between a lateral switch and an equilateral switch, but is biased heavily toward a lateral switch configuration. This also helps the curved switch point at the expense of the straight switch point by lining up wheels for the diverging route curve prior to the switch point. This contributes to the good wear performance of the SEPTA switches.

The NUCARS™ simulations suggest that the best replacement for the SEPTA Number 8 spiral switch turnout would be a modified AREMA Number 8 turnout with a housed switch point, a tangential entry to the switch, a switch rail with a radius of 372 ft, and the closure rail of the same radius as the switch rail. The lead length of this turnout is 59 ft, but the frog is larger than a Number 8. This turnout produces smooth steering of B-IV cars for both the facing point and trailing point runs. Wheel lateral loads are comparable to the SEPTA turnout at low speeds and are lower at higher speeds. Unlike the SEPTA turnout, the increase in lateral loads is quite gradual—from 5 to 25 mph. This change in the maximum wheel lateral loads from 5 mph to 25 mph

is less than 20%. The improved ride quality for this replacement turnout is also evident from smaller car body lateral and yaw accelerations, reduced axle lateral and yaw accelerations, lesser vertical unloading and loading of the wheels, and lower *L/V* ratios. Further, the improved ride quality gives tread and flange wear indices that are generally uniform through the turnout curvature, thereby indicating even wear and probably a longer life for this replacement option.

Phase II of this project will develop a replacement switch for the SEPTA spiral design. The aforementioned modified AREMA switch will serve as the starting point for this design.

CHAPTER **1**

INTRODUCTION

Transit switch designs in the early 1900s were quite sophisticated by today's standards, with features that have been rediscovered and are being implemented in modern high-speed switch designs. These switches gave excellent service for many years, often outliving the lower cost but simpler replacement designs that followed. Many of the designs became obsolete because most were unique to a particular transit company and, in some cases, casting patterns were no longer available.

TCRP members observed that often the best performing switches on their systems were the oldest switches. The original tangential and spiral geometry switches often had service lives of 50 years or more. Additionally, these switches would outlive their replacement designs by 100 to 1,000%.

The switches produced in the 1900s share some or all of the following features:

- Tangential geometry (no entry kink angle);
- Spiral geometry (variable switch curvature);
- Housed switch points;
- Austenitic Manganese Steel (AMS) switch points and stock rails;
- Guard rails in front of the switch; and
- Guard rails in the switch.

The Switch Design Evaluation Technical Advisory Group (TAG) selected a design used by the Southeastern Pennsylvania Transit Authority (SEPTA) as a representative of a good performance switch design. Table 1 lists the features of the SEPTA spiral switch turnout compared with an American Railway Engineering Maintenance of Way Association (AREMA) Number 8 lateral switch turnout. The objectives of the two switch designs are clearly different. The SEPTA switch turnout is built for ride quality with smoothed transitions and spiral curves to minimize the rate of change of accelerations. The AREMA switch turnout is built for economy, speed, and component durability. By having a large kink (entry) angle and large radius closure curve, the design geometry of the AREMA switch turnout maximizes allowable speed under the "cant deficiency" rule—the Federal Railroad Administration's (FRA) rule for speed in curves. The SEPTA switch turnout designers were not subject to this rule; thus minimum switch closure curve radius and maximum cant deficiency were not important issues for them.

Figure 1 compares the layouts of the SEPTA and the AREMA switches. The geometry and alignment differences can be seen from this plot. The SEPTA switch spiral geometry produces a lower entry angle for facing point and a lower exit angle for trailing point movements.

1.1 SEPTA SWITCH INSPECTION

On May 23, 2000, Transportation Technology Center, Inc. (TTCI) and SEPTA track engineering personnel inspected a SEPTA spiral geometry switch at Erie Avenue on the Broad Street Subway line based in Philadelphia, Pennsylvania. The switch was measured for gage, cross level, and running surface profiles to be used in the switch design modeling effort. A total of 25 profiles were measured through the diverging route of the switch and were used to develop the vehicle track dynamics model of the switch. An accurate representation of the track running surface is essential in the simulation. Profiles were measured at 24-in. intervals throughout the diverging route switch point. Additional measurements were made for 10 ft in front of the switch point. Profile measurement spacing was reduced to 6 in. in the critical point of switch area where running surface changes are more abrupt. Near the point of switch, the profile included the stock rail running surface as well.

Table 2 lists the locations of the measurements, as well as the corresponding gage error and cross level. The gage error as listed is defined as the difference between the left rail lateral perturbation and right rail lateral perturbation. A plus (+) value indicates a wide gage, while a minus (–) value indicates a tight gage. Similarly, cross level is defined as the difference between the left rail vertical perturbation and the right rail vertical perturbation. The signs of cross levels given in the table are for the facing point runs such that a plus value indicates that the left rail is higher and a minus values indicates that the right rail is higher. The signs for the trailing point runs will be opposite to those shown in the table. As can be seen, a wide gage exists all through the turnout. Gage error is greatest near the point of switch at

TABLE 1 Comparison of SEPTA and base case turnout designs

Switch Design Feature	SEPTA	AREMA Number 8
Type	Lateral	Lateral
Lead Length	57 feet	59 feet
Geometry: Entry Angle	Tangential	Non-Tangential
Geometry: Curvature	Spiral (840-210 feet)	Curve (616.55 feet)
Allowable speed (cant deficiency rule)	12.5 mph	20.3 mph
Point: Configuration	Housed	Undercut
Point: Material	AMS casting	Rail steel
Point: Guarding	Yes	No
Closure Curve Guarding	Yes	No

about 1 in. This is because of the design vertical and lateral point slopes and some wear. The point slopes create a short distance "hole" in the gage face. Wheels will span this hole with little effect. Also a full riser height of 0.125 in. is apparent in the table.

The condition of the switch points, stock rails and closure rails, all installed in 1926, was very good overall. Profiles of the diverging route switch point and stock rail show that they have very little wear and flow after many years in service. Figures 2 and 3 show a cross-section running surface profile and photographs of the switch at various locations.

The cross-section profile shown in Figure 2 is taken at the point of switch. The profile indicates the type of wear seen in the switch point/stock rail pair. The switch point gage face largely conforms to moderately worn wheel flanges. There is metal flow to the field side of the stock rail as indicated by the squared corner and vertical field side railhead. This profile also shows the amount of point depression remaining. The switch point is approximately $^{7}/_{64}$ to $^{1}/_{8}$ in. below the stock rail crown here. The original point depression was $^{1}/_{4}$ in. in $12^{1}/_{2}$ in. in 1926. The design switch riser was $^{1}/_{8}$ in., reaching this height at 90 in. from the point of switch. The small "bump" in the stock rail running surface seen just to the field side of the center of the rail is not actually there; it is an artifact of the way the profile is measured. The profile is measured in two parts—gage side part and the field side part—with the bump being a slight misalignment of the two halves. Such discontinuities were eliminated in the profiles used in the dynamic simulation.

As the photographs of the point of switch show (Figures 3 a and b), there was no deformation in the area where wheels strike the point. There is also little wear on the switch point in

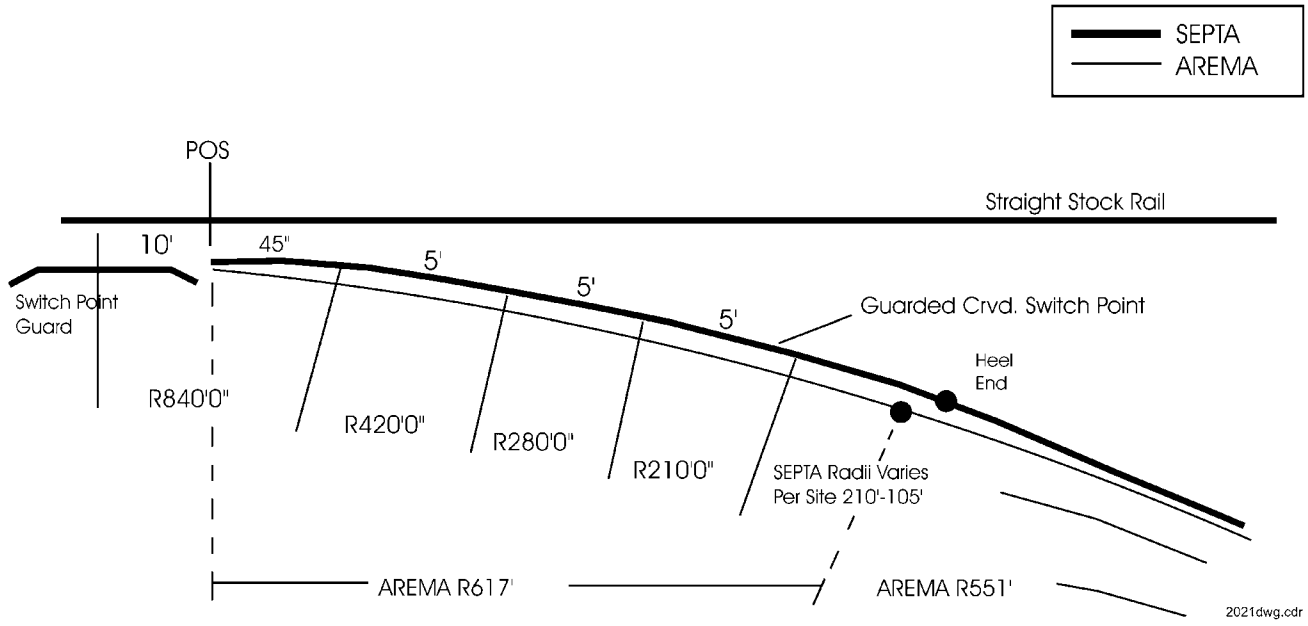

Figure 1. SEPTA and AREMA switch geometry (plan view).

TABLE 2 Location of switch point profile measurements

Location from POS (feet)	Feature	Gage Error (inches)	Cross Level (inches)
-10	Start guard	0.375	-0.0625
-8		0.3125	-0.0625
-6		0.3125	-0.125
-4		0.375	-0.125
-2		0.4375	-0.0625
-1		0.625	0.0625
-0.5		0.625	0.0625
0	Point of switch	1.0	0.125
0.5		1.0	0.125
1		0.875	0.125
1.5		0.875	0.125
2		0.8125	0.125
4		0.8125	0.125
6		0.75	-0.125
8		0.625	-0.25
10		0.5	-0.25
12		0.375	-0.25
14		0.375	-0.125
16	Heel	0.375	-0.125
18		0.25	-0.125
20		0.125	-0.0625
22		0.25	0.0
24		0.4375	0.125
26		0.375	0.125
32		0.4375	-0.125

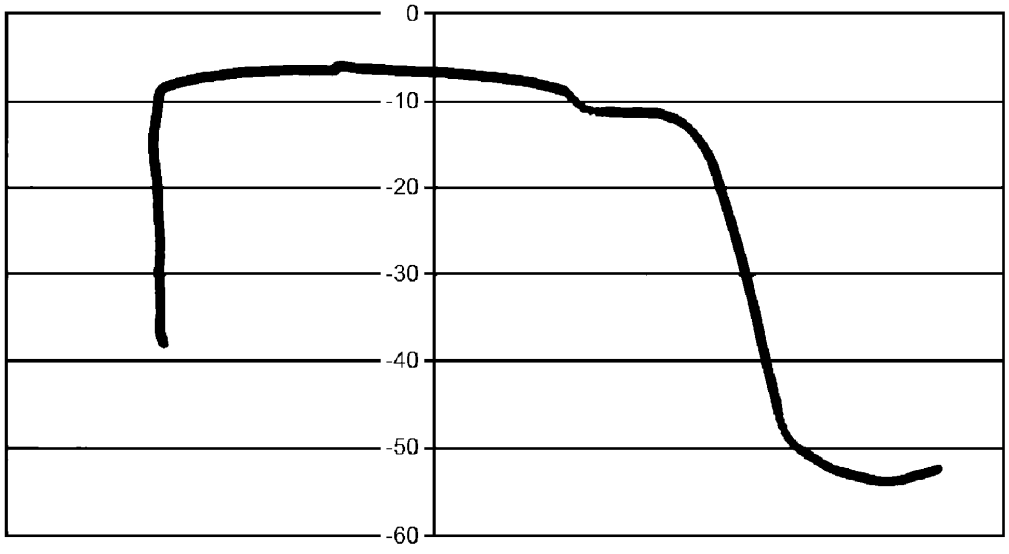

Figure 2. Switch point running surface profile at the point of switch.

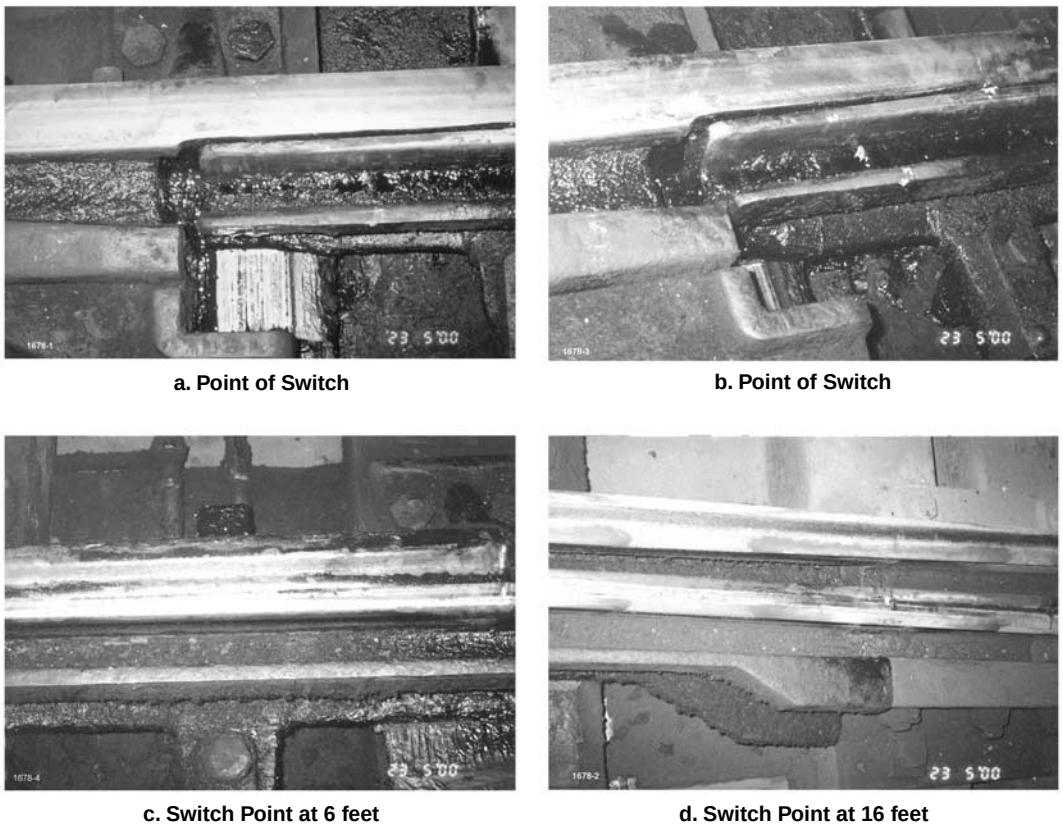

a. Point of Switch

b. Point of Switch

c. Switch Point at 6 feet

d. Switch Point at 16 feet

Figure 3. Erie Avenue switch inspection: point of switch (a and b), at 6 feet (c), and at 16 feet (d).

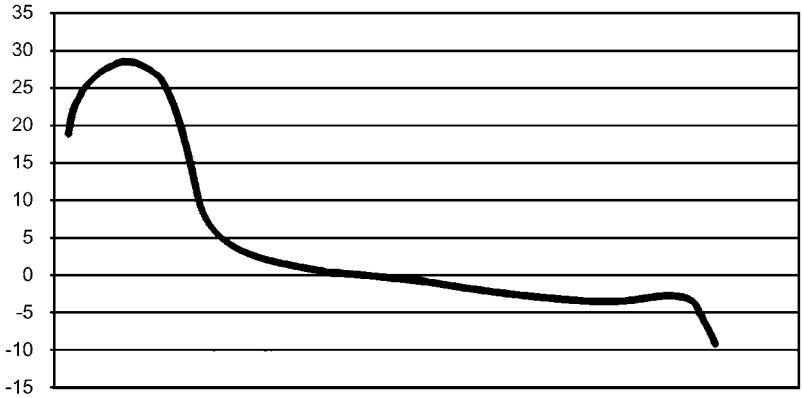

Figure 4. Typical worn SEPTA B-IV car wheel profile.

the first 2 ft as is typically seen in tangential switches. This indicates that the turnout has good alignment both horizontally and vertically. The third photograph (Figure 3c) shows an area where the switch point riser is at its full height of about 1/8 in. above the stock rail. The hollowed portions of wheel treads would cross the stock rail at this location. The characteristic blending of the stock rail and switch point running surface wear bands can be found in this location.

TTCI verified that the switch point and stock rail were from the original installation in 1926 from the rolling dates on the rails in the turnout.

1.2 WHEEL INSPECTION

Worn wheel profiles were measured at the car shop that maintains the cars running over the measured switch. Ten in-service wheels were measured to produce a representative profile for modeling. Figure 4 shows a profile from this database. The wheels were all similar in shape with various amounts of wear and had relatively good profiles with minimal flange wear and tread hollowing. A wheel profile with a moderate amount of wear was selected to represent the B-IV car wheels for the vehicle track dynamics model.

CHAPTER 2

NUCARS™ MODEL DEVELOPMENT

TTCI's NUCARS is a vehicle-track dynamic simulation program *(1)* used extensively by the railroad industry to develop car and special track work designs. The NUCARS program reads input data from a file defining mechanical characteristics of the vehicle and from a file defining the geometry of the track to be simulated. The file of vehicle mechanical characteristics is referred to as a vehicle model, and the file containing track geometry is referred to as the track model. These models are discussed in the following sections.

2.1 VEHICLE MODEL

The NUCARS™ vehicle model was created using SEPTA B-IV D/E car characteristics. The B-IV cars, equipped with four powered axles, were built by Kawasaki. The cars have H-frame trucks, chevron primary suspension, and secondary air suspension. The principal dimensions of the car per Drawing No. 9400010, "General Arrangement (D/E)," are as follows:

- Car length over couplers: 67 ft 10 in.;
- Car width: 10 ft;
- Car height: 12 ft $2^{3}/_{32}$ in.;
- Floor height: 4 ft 2 in.;
- Rigid wheel base: 6 ft 10 in.;
- Wheel diameter: 28 in.; and
- Truck centers: 47 ft 6 in.

An empty car weight of 72,600 lb and loaded car weight of 108,664 lb were used to calculate the required car body mass and mass moment of inertias for the vehicle model.

The information provided on 120-deg V-Chevron springs *(2)*, arranged 11 deg from the vertical, was used to provide connections between the H-frame trucks and the axles. One pair of V-springs per journal was used to provide the following characteristics:

- Vertical stiffness: 8,900 lb/in.,
- Longitudinal stiffness: 106,000 lb/in., and
- Lateral stiffness: 17,000 lb/in.

The design vertical static loads per journal were defined as follows:

- 7,161 lb (empty car at about 3.5 Hz);
- 8,530 lb (all seats occupied, no standees at about 3.2 Hz);
- 9,848 lb (load for endurance calculation); and
- 11,669 lb ("crush load," maximum load for strength).

Given that dynamic stiffness would be higher by about 25% to 45% than the static stiffness, a dynamic "crush load" of as much as $1.45 \times 11{,}669 = 16{,}920$ lb per journal is sustainable.

The secondary suspension provided between the car body and the bolsters used air bags. The air bags help in providing noise control; leveling to maintain floor height; keeping the car body natural frequency constant; and providing isolation from bounce, pitch, and car body vertical bending frequencies. The properties derived from an equivalent mechanical system were used in the vehicle dynamic model.

Other components of the vehicle model were side bearing pads, vertical wear sleeves at center pins, traction rods, lateral bump stops, inclined lateral shock absorbers, vertical shock absorbers, and the wheel-rail connections. Overall, 12 bodies and 60 connections were used to assemble the vehicle's dynamics model for the NUCARS™ simulation. The NUCARS™ vehicle model was simplified by using non-powered trucks. Although the use of powered trucks may change the magnitude of lateral loads, it should not materially affect relative comparisons of switch designs.

2.2 TRACK MODELS

The track model comprises track geometry data and the track curve data. The track geometry data is used to specify perturbed track input to the model and consists of lateral and vertical perturbation amplitudes of each rail at some specified positions along the track. The track curve data, on the other hand, is used for specifying superelevation and the curvature information of the track.

For all switch designs, the switch is modeled as a turnout: through the closure rails and a straight (tangent) frog so that trailing axles may operate through the switch. Track beyond the frog extends as tangent from the frog along the frog angle to the main line. The length of the SEPTA vehicle is such that the leading truck of a car is on the frog when the trailing truck

is on the switch. This track configuration, essentially a turnout with a moveable point frog, allows full analysis of vehicle performance on the switch while minimizing the effects of the frog or track layout beyond the frog.

Thus, all simulations were done using this type of turnout model to analyze the effects of switch design features. The term "turnout" will be used to describe the track models analyzed in the report.

2.2.1 SEPTA Turnout

The SEPTA tangential design spiraled geometry switch is in a Number 8 lateral turnout. It has a spiral geometry (840 ft to 210 ft). The alignment, gage, cross level, and vertical profile in NUCARS™ were modeled according to inspection measurements made by TTCI personnel. The track curvature information was used from Drawing No. V-97163 and Drawing No. 7-W-16984, both provided by SEPTA *(3, 4)*. Track models for both the facing point diverging right and trailing point diverging left moves were made. This case is designated as "SEPTA As-is."

A variation of the SEPTA switch with a nontangential geometry was also developed to simulate conditions somewhat similar to the AREMA design. This was done by introducing an entry (kink) angle in the track curve data. Introduction of an entry angle equal in magnitude to that of the AREMA design entailed changing the SEPTA switch turnout curvature geometry substantially. This option on the equality of entry angle magnitudes was therefore abandoned. Instead, it was decided that a change should only be made in the 840-ft-radius arc and that the rest of the switch curvature data should not be changed. Drawing No. V-97163 shows that the point of switch is 6 ft from the beginning of the 10-ft-long 840-ft-radius arc when looking in the facing point direction. A kink angle having a magnitude of 8′11″ (0.1364 deg) was introduced at the point of switch. The radius of the remaining 840-ft arc, following the point of switch, was then changed to 1680 ft. The rest of the original curve data was used. In this manner, the lead length equal to that of the SEPTA As-is turnout was maintained. This case is designated as "SEPTA-Kink."

2.2.2 AREMA Replacement Turnout

The comparison switch used for the design analysis is the nontangential, AREMA Number 8 lateral turnout with curved split switch and uniform risers *(5)*. The length of the switch rail is 13 ft with a switch radius of 616.55 ft corresponding to Point Detail No. 5100 per *Portfolio of Trackwork Plans of AREMA*. The top cut is 6 ft and the full riser height is 1/4 in. The angle at point (entry angle or kink angle) is 1 deg, 41 min., 31 sec. (1.692 deg). The curved closure rail is 41.05 ft long and has a radius of curvature of 550.75 ft. The actual lead, equal to the distance between the point of switch and 1/2-in. point of frog, is 58 ft, 11 1/8 in.

The track geometry data and the track curve data were modeled as they would be for a new AREMA Number 8 turnout. This case is designated as "AREMA As-is." Track models for both the facing-point diverging-right and trailing-point diverging-left moves were made.

Again, to identify and evaluate the performance due to changes in the design features, four different variations of the AREMA Number 8 turnout were developed to compare their performance with the SEPTA switch. These four variations are as follows:

- Tangential AREMA Number 8 turnout (without entry angle) designated as "AREMA-Case 1."
- Tangential AREMA Number 8 turnout with switch and curved closure rail radii of 372 ft to give a lead length equal to that of the AREMA As-is turnout. This case is designated as "AREMA-Case 2."
- Tangential AREMA Number 8 turnout with curved closure rail of same radius as switch rail radius designated as "AREMA-Case 3."
- Nontangential AREMA Number 8 turnout with curved closure rail of same radius as switch radius designated as "AREMA-Case 4."

Table 3 lists the features of the design variations described.

2.3 WHEEL/RAIL CONTACT MODEL

The wheel/rail contact model describes the contact between the wheels and the rails. This description is provided for various lateral positions (shifts) of the wheelset relative to the rails. In addition, contact geometry is defined as a function of distance along the track. Even though the SEPTA switch has AMS casting points and the AREMA switch has rail steel points, a distinction regarding steels is not made in the contact model.

Positions of contact between the wheelset and rails for various shifts of the wheelset relative to the rails are calculated using the profile geometry of each wheel; the wheels' radii; the back-to-back spacing of the wheels and the profile shapes of the two rails, their cant angle, and the track gage. Corresponding to each contact position, the pertaining geometric parameters (e.g., wheelset roll angle, rolling radii difference, contact angles, and contact areas) are calculated based on the assumptions of the Hertzian contact between the wheels and rails. By defining these at various locations along the turnout, the wheel/rail contact model all through the switch is thus defined. Between any two consecutive locations along the track, the contact model defined for the first location is used.

TABLE 3 Features of modeled switch/turnout design variations

Design Name	Design Description	Lead Length (feet)	Entry Angle (degrees)	Switch Curve Type	Switch Radius (feet)	Closure Curve Radius(feet)	Allowable Speed *(6)* (mph)
SEPTA-as built	Tangential Spiral	57	0	Spiral	840	210	12.5
SEPTA Kink	Secant, Spiral	57	0.1364	Circular and Spiral	1,680	210	12.5
AREMA (Plan No. 920-51)	Secant, Circular	59	1.692	Circular	616	551	20.3
AREMA Case 1	Tangential, Circular	73	0	Circular	616	551	20.3
AREMA Case 2	Tangential, Circular, Balanced *(7)*	59	0	Circular	372	372	16.7
AREMA Case 3	Tangential Circular Balanced	76	0	Circular	616	616	21.5
AREMA Case 4	Secant Circular Balanced	60	1.692	Circular	616	616	21.5

2.3.1 SEPTA Turnout

The 25 measured running surface (rail) profiles of the track (Section 1.1) and the representative wheel profile (Section 1.2) were used to determine the contact geometry between the wheelset and the different rail profile combinations through the switch and turnout. These contact geometries thus provided the actual operating contact conditions through the diverging route of the switch and turnout.

2.3.2 AREMA Turnout

The wheel/rail contact model for the AREMA route was calculated by using the representative wheel profile of Section 1.2 and the new 136RE 10-in. crown rail profiles for the switch point and stock rail pair. A rail cant of 1 in 40 was also used. A larger number of contact geometries along the track were calculated for the top-cut region of the switch to properly simulate the contact conditions in this area where running surface changes are more severe.

CHAPTER **3**

PARAMETRIC STUDY OF SWITCH/TURNOUT DESIGN FEATURES

Variations in design parameters for the study include tangential and nontangential entry to the switch and the changes in the radii of the switch and curved closure rails. The effect of speed on various designs, for both the facing-point diverging-to-right runs and the trailing-point diverging-to-left runs, was evaluated and compared with the SEPTA As-is turnout and a new AREMA Number 8 turnout. Maximum lateral loads, maximum wheel *L*/*V* ratios, maximum sum (axle) *L*/*V* ratios, minimum wheel/rail vertical loads, maximum lateral accelerations, and the wear indices were factors in assessing design performance.

Of the various replacement designs listed in Table 3, two options have lead lengths more or less equal to the SEPTA turnout: the AREMA Number 8 per Plan No. 920-51 (AREMA As-is) and the AREMA-Case 2. Both AREMA options have a lead length of about 59 ft and circular curvature geometry. The AREMA per Plan has an entry angle while Case 2 is tangential. Based on this information, these two designs are the most practical replacement options. As such, this report focuses on the performance comparisons of the B-IV cars through the SEPTA As-is turnout and these two AREMA replacement options.

3.1 LATERAL LOADS

Figures 5 and 6 show maximum lateral loads exerted on the left wheel of Axles 1 and 3 for facing-point diverging-right runs at 5 to 25 mph. The negative values seen are a result of the sign convention used in the NUCARS™, indicating that the exerted lateral load on the left wheel is toward the right side for the facing point runs.

Very high lateral loads arise due to track curvatures of the AREMA As-is and AREMA-Case 4 turnouts—as much as 20,100 lb on the left wheel of Axle 1 at 25 mph for the AREMA As-is turnout. Even for lower speeds, these loads are quite high. The SEPTA As-is switch curvature also generates high lateral loads on the left wheel of Axle 1 for speeds greater than 15 mph—as much as 17,500 lb at 25 mph. Comparatively, the curvature layout of AREMA-Case 2 turnout exerts a maximum lateral load of 13,500 lb each on the left wheel of both Axles 1 and 3 at 25 mph. Moreover, the exerted lateral loads for this turnout increase rather gradually from 5 to 25 mph. As such, this gradual change in the maximum lateral loads from 5 to 25 mph is only about 20% for the left wheel of both Axles 1 and 3 in the facing-point diverging-right runs.

Figures 7 and 8 show maximum lateral loads exerted on the right wheel of Axles 1 and 3 for trailing point diverging left runs. The positive values in these figures indicate that the exerted lateral load on the right wheel is toward the left side for these runs. The exerted lateral loads are quite comparable between the AREMA As-is and AREMA-Case 2 turnout curvatures for both Axles 1 and 3 from 5 to 25 mph; lateral loads are within 8% of each other for Axle 1 and within 13% of each other for Axle 3. Also, as against the sudden increase in the lateral loads for the SEPTA As-is turnout for speeds greater than 15 mph, the lateral loads increase gradually for the AREMA As-is and AREMA-Case 2 turnouts in the trailing point runs. This increase is less than 17% for Axle 1 and less than 19% for Axle 3. For AREMA-Case 2, the highest lateral load (18,000 lb) occurs on Axle 1 at 25 mph. For the AREMA As-is design, the highest lateral load (16,000 lb) occurs on Axle 3 at 25 mph.

As seen in these figures, the "cutoff" speed between the best and worst performance for the SEPTA As-is turnout is 15 mph. Of all the designs considered, SEPTA As-is performs best below 15 mph and worst above 15 mph in the trailing point runs in terms of lateral load. For the right wheel of Axle 1, the increase in lateral load is 7% between 5 and 15 mph while an increase of about 44% occurs from 15 to 25 mph. For the right wheel of Axle 3, these increases are about 23% and 79.5% for the 5 to 15 and 15 to 25 mph speed ranges, respectively. The highest lateral load exerted is 21,700 lb on the right wheel of Axle 3 at 25 mph.

Figure 9 shows histories of wheel lateral loads with respect to distance (distance refers to the first axle) through the SEPTA As-is, AREMA As-is, and AREMA-Case 2 turnouts at 25 mph. Figure 10 provides these histories at 15 mph. A comparison of these two figures shows that the lateral load characteristic behavior of a B-IV car through a particular turnout remains basically the same at both low and high speeds. Only the magnitudes of the exerted lateral loads differ: they are lower at low speeds. Also the adverse effect from the "kink" angle at the point of switch is reduced substantially at lower speeds. The parametric study with respect to speed

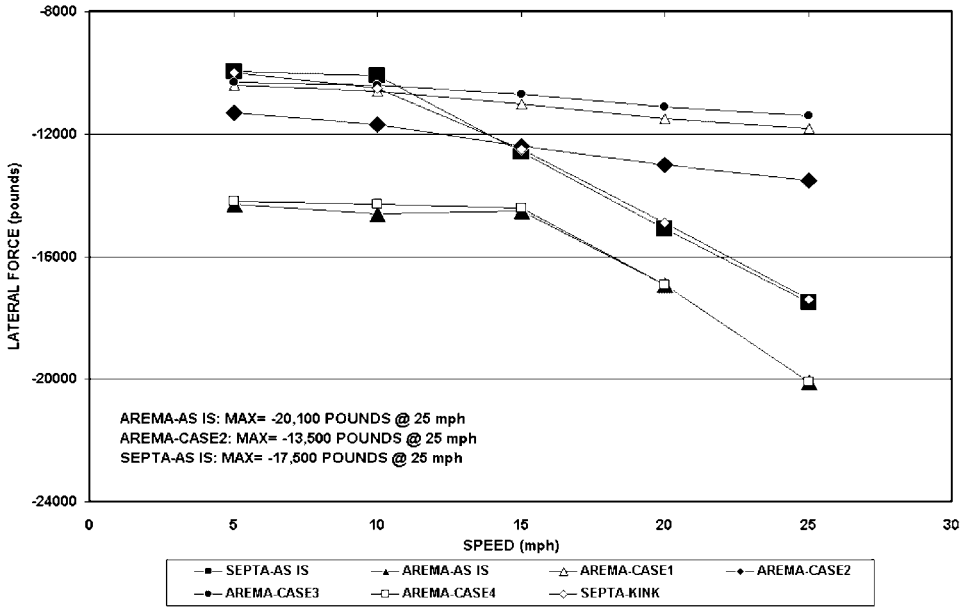

Figure 5. Lateral load comparison between SEPTA and AREMA turnouts: left wheel, axle 1, facing point diverging right runs.

was conducted up to the possible 25 mph for these cars in the diverging runs. As the worst behavior is expected at higher speeds, the behavior of a B-IV car at 25 mph through the various turnouts is the one that is comparatively analyzed below.

As shown in Figure 9, the first lateral load spike for the facing point run through the SEPTA As-is turnout occurs when Axle 1 is just past the point of switch at 156 ft, and then at about 210 ft after exiting from the "spiral-out" radius of 420 ft of the turnout. The car body acting as a rigid chord of the track curvature forces the left wheel of Axle 3, on the other hand, to achieve its first maximum while still on the tangent portion before the point of switch. Axle 3 appears to achieve a radial position beyond this point except when exiting the "spiral-out" radius of 420 ft and achieves another maximum then. Back and forth lateral bumping on and off of the left rail of the wheels of Axles 1 and 3 is apparent from the maximum and minimum locations of the wheel loads in this figure. A smooth steering through the turnout is not obvi-

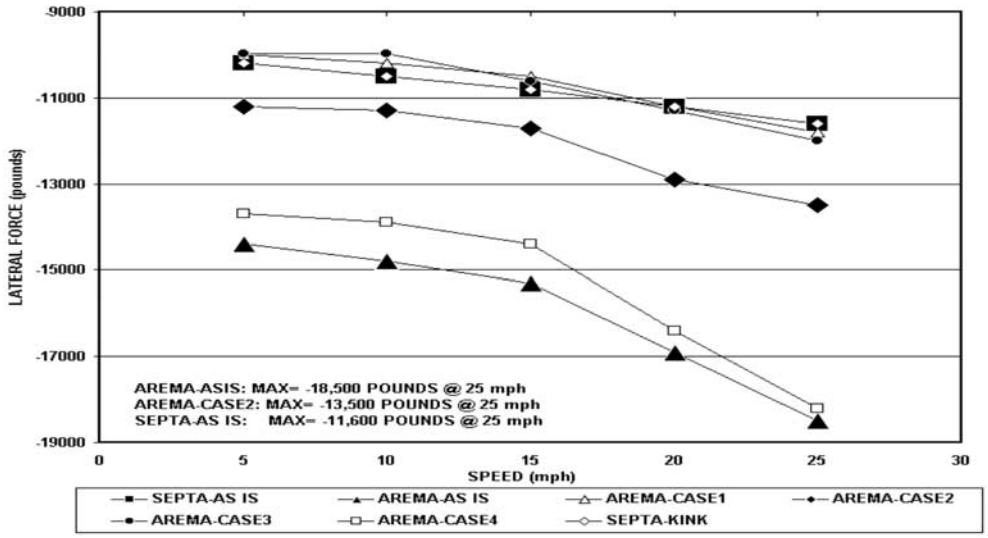

Figure 6. Lateral load comparison between SEPTA and AREMA turnouts: left wheel, axle 3, facing point diverging right runs.

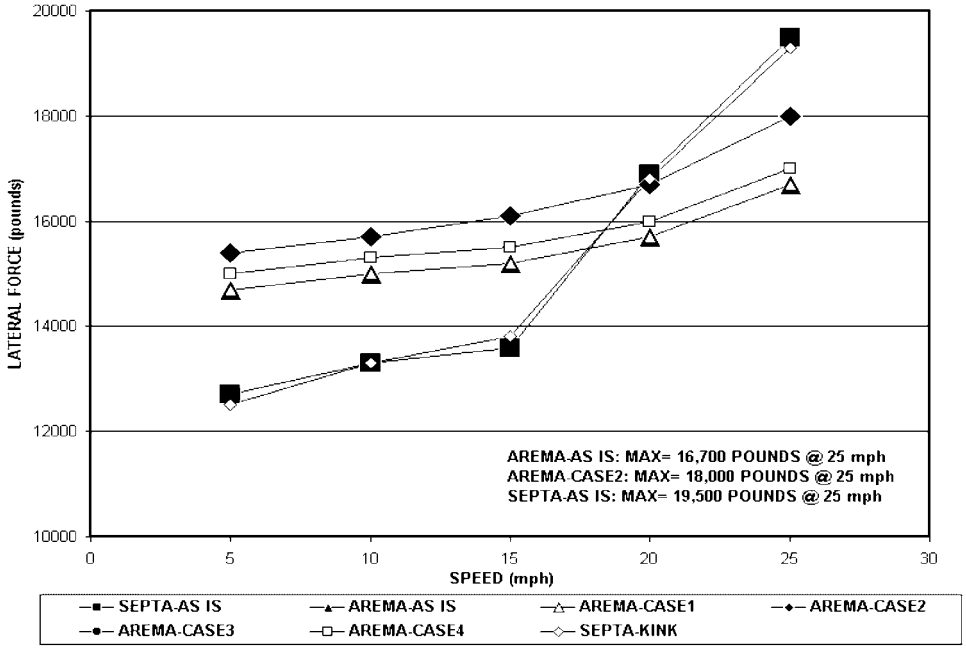

Figure 7. Lateral load comparison between SEPTA and AREMA turnouts: right wheel, axle 1, trailing point diverging left runs.

ous from these plots and is probably attributable to the tightness of the spiral geometry of this turnout with respect to the long truck centers and wheelbase of the car.

This "spiral tightness" of the SEPTA As-is turnout is also obvious from the lateral loads exerted on the right wheels in the trailing point run shown in Figure 9. A series of striking the right rail and then bouncing off it, starting right from the entry to the spiral at about 100 ft, is obvious in these plots of the lateral loads on the right wheels. Location of the point of switch is at 144 ft for the trailing point runs. Lateral load spikes for the right wheel of both Axles 1 and 3 therefore correspond to the abrupt change in curvature about the point of switch location. Rapidly changing axle yaw to accommodate various radii of the track curvature together with car body

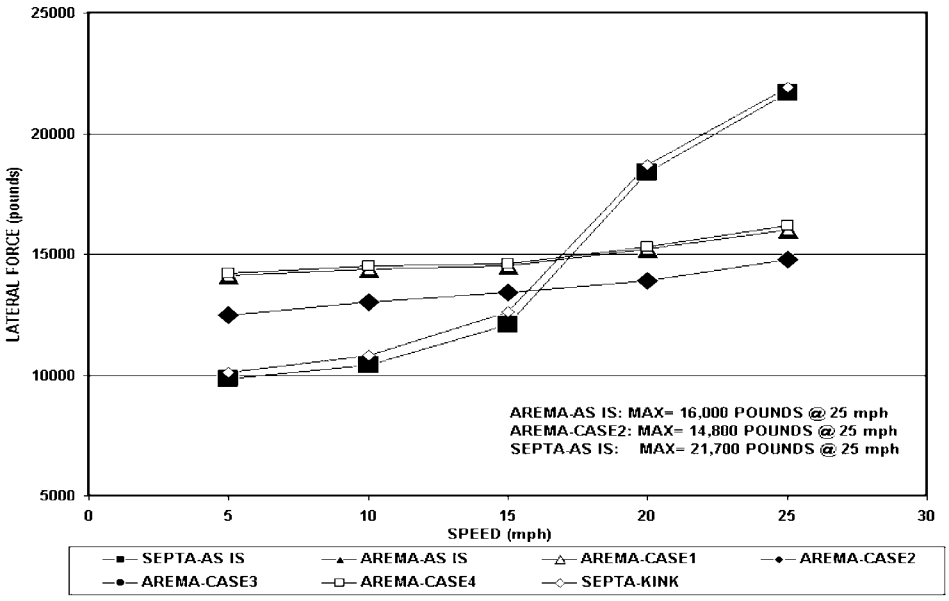

Figure 8. Lateral load comparison between SEPTA and AREMA turnouts: right wheel, axle 3, trailing point diverging left runs.

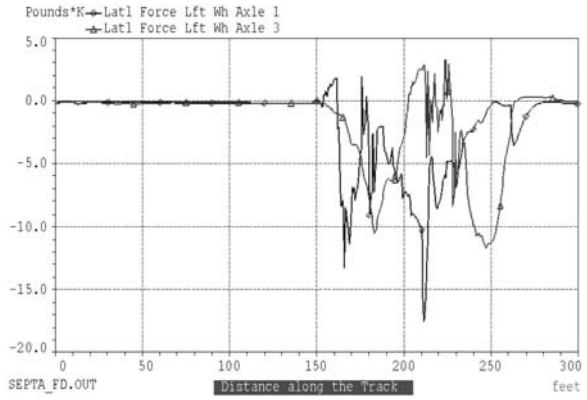

Left Wheel Axles 1 & 3, Facing Point SEPTA As-is, Point of Switch = 156 feet

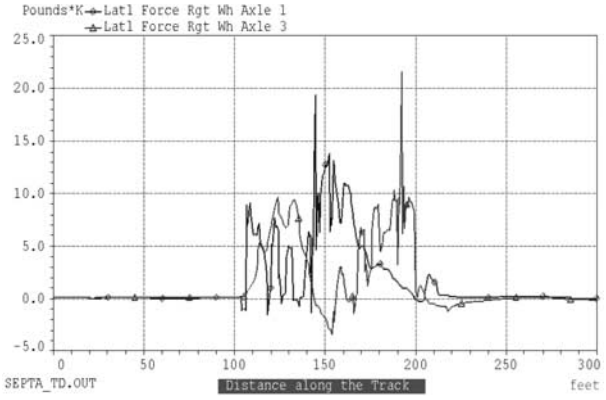

Right Wheel Axles 1 & 3, Trailing Point SEPTA As-is, Point of Switch = 144 feet

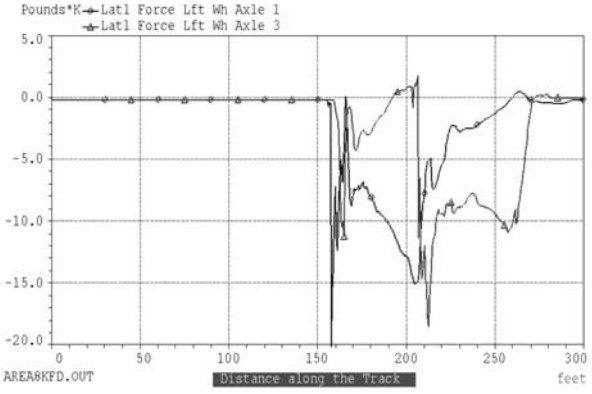

Left Wheel Axles 1 & 3, Facing Point AREMA As-is, Point of Switch = 156 feet

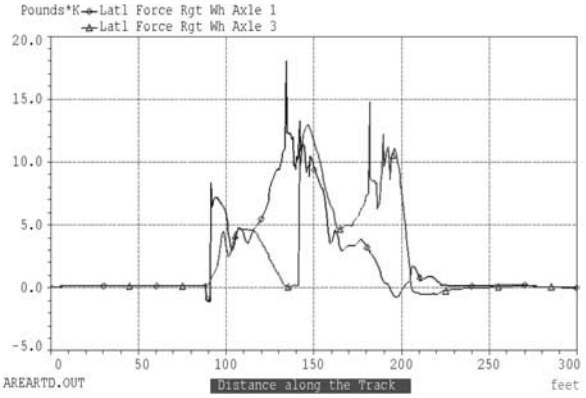

Right Wheel Axles 1 & 3, Trailing Point AREMA As-is, Point of Switch = 144 feet

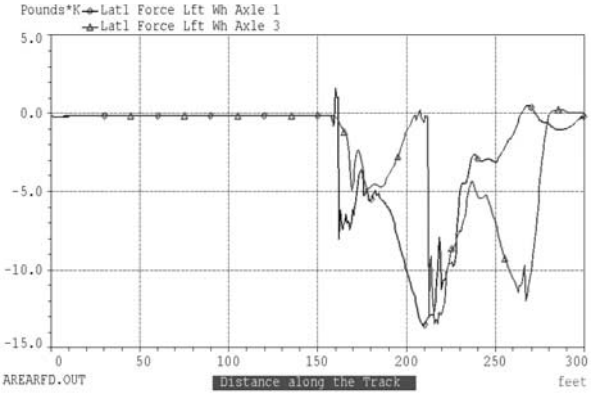

Left Wheel Axles 1 & 3, Facing Point AREMA-Case 2, Point of Switch = 156 feet

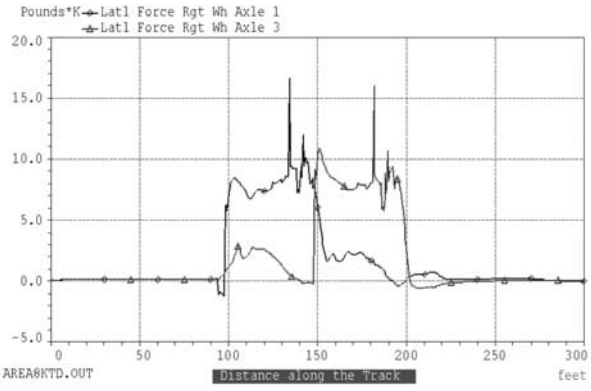

Right Wheel Axles 1 & 3, Trailing Point AREMA-Case 2, Point of Switch = 144 feet

Figure 9. Lateral loads on left and right wheels of axles 1 and 3 at 25 mph.

twist are probably the reasons for the steering "turbulence" obvious in these lateral load plots.

Again, as shown in Figure 9, the "signatures" of lateral load exerted on the wheels of both Axles 1 and 3 with respect to distance are mostly similar for the AREMA As-is and AREMA-Case 2 turnouts, except at the location of the point of switch in the facing point runs. The effect of the "kink" angle is negligible in the trailing point runs. The lateral load spikes seen for the trailing point runs in this figure are due to the change from a finite radius of curvature to an infinite radius of curvature. In the facing point runs, the presence of the "kink" angle greatly adds to the effect produced by change

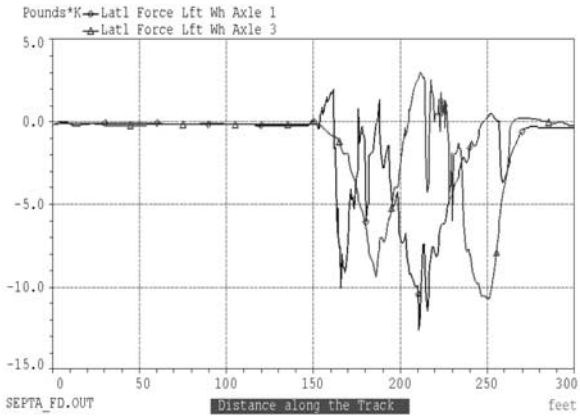

Left Wheel Axles 1 & 3, Facing Point SEPTA As-is, Point of Switch = 156 feet

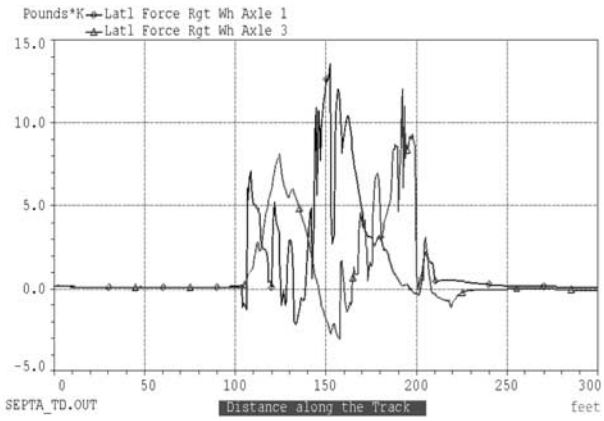

Right Wheel Axles 1 & 3, Trailing Point SEPTA As-is, Point of Switch = 144 feet

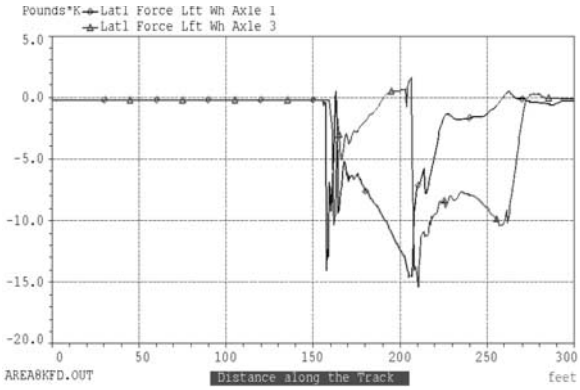

Left Wheel Axles 1 & 3, Facing Point AREMA As-is, Point of Switch = 156 feet

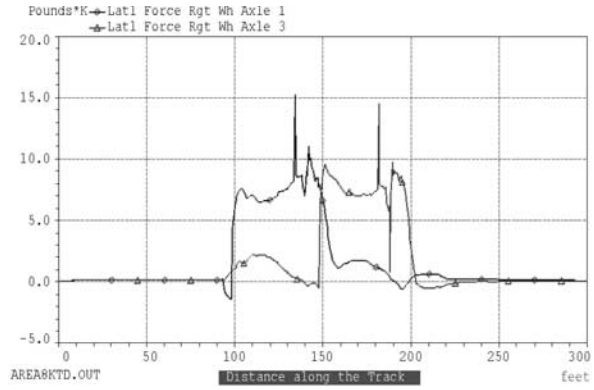

Right Wheel Axles 1 & 3, Trailing Point AREMA As-is, Point of Switch = 144 feet

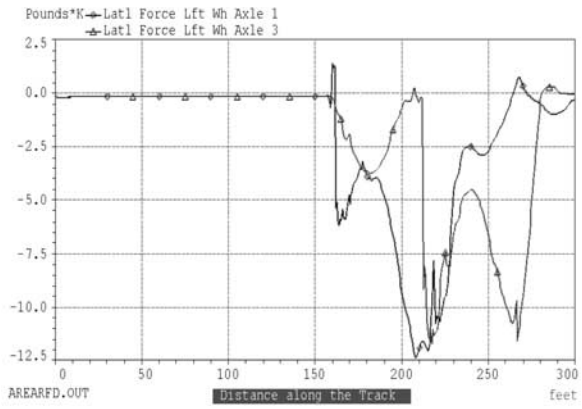

Left Wheel Axles 1 & 3, Facing Point AREMA-Case 2, Point of Switch = 156 feet

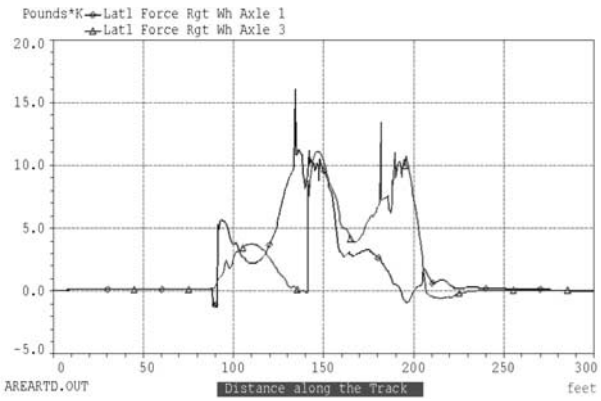

Right Wheel Axles 1 & 3, Trailing Point AREMA-Case 2, Point of Switch = 144 feet

Figure 10. Lateral loads on left and right wheels of axles 1 and 3 at 15 mph.

in the curvature at the point of switch. A comparison of lateral loads between AREMA As-is with kink angle and the AREMA-Case 2 without kink angle, shows that the sudden change in direction due to the "kink" angle can increase lateral loads in the vicinity of the point of switch as much as 3 times when the kink angle is present.

On the other hand, a comparison with the SEPTA turnout shows that the progression of exerted lateral loads on wheels through the curvatures of these AREMA turnouts is more predictable. As an example, the sudden change in direction due to the kink angle that produces a sharp lateral load spike for the left wheel of Axle 1 in the facing point run. However,

the wheel quickly recovers and then resumes a rather smooth steering through the switch rail and closure rail curves generating gradually increasing lateral loads due only to the curvature effect till exiting to the tangent portion at the frog. The left wheel of Axle 3 follows the same pattern. In trailing point runs, a smoother negotiation of B-IV cars through the curvature of the AREMA As-is turnout than those of the SEPTA As-is and AREMA-Case 2 turnouts is obvious. The radii of curvature of the AREMA As-is turnout are larger. Also, the individual curve lengths in it are longer; therefore, the car body chord effect does not seem to affect the lateral loads for this turnout unduly, although a marginal chord effect is apparent for the AREMA-Case 2 turnout due to a few erratic changes in the lateral loads for this turnout.

To summarize, comparable lateral wheel loads at speeds lower than 15 mph and lower lateral wheel loads at speeds greater than 15 mph, with respect to the SEPTA As-is turnout, are generated for the AREMA-Case 2 turnout. Further, there is evidence of smoother steering through the AREMA-Case 2 turnout than through the SEPTA As-is turnout. The switch, with its larger radius closure curve, does not suffer as much from the adverse effects of a tight curvature: car body twist, the chord effect and rapidly changing axle yaw. From the study of lateral loads, it therefore appears that the AREMA-Case 2 design could be a good replacement option for the SEPTA As-is turnout.

3.2 ACCELERATIONS

With respect to the lateral and yaw accelerations of Axles 1 and 3 at 25 mph, Figures 11 through 13 depict an "agitated" negotiation of the B-IV cars through the SEPTA As-is turnout against the rather "quiet" negotiation of the same cars through both the AREMA As-is and AREMA-Case 2 turnout curvatures. Figures 14 through 16 show that a similar conclusion can be derived at lower speeds from a comparison of these accelerations at 15 mph. A comparison of lateral and yaw accelerations of the axles at 15 and 25 mph also shows that the characteristic behavior of the B-IV cars through a particular turnout curvature remains the same at low and high speeds. In particular for the SEPTA As-is turnout, it is apparent that at the lower speed of 15 mph many changes in axle yaw acceleration occur in order to accommodate various curvatures, but these changes are not very severe. Also, it may be noted from Figures 11, 12, 15, and 16 that the high acceleration spikes, associated with the change from infinite radius of the tangent track to the finite radius of the curved track, are either eliminated or dramatically reduced at lower speed. This behavior is clearer for trailing point runs.

A comparison of the responses of the B-IV car at the highest possible speed of 25 mph through these turnouts shows that, except in the neighborhood of the point of switch and/or while transiting from an infinite radius of the tangent track to the finite radius of the turnout curvature, axle lateral and yaw accelerations for both the AREMA As-is and AREMA-Case 2 turnouts are very small in magnitude in both the facing and trailing point runs. Also, these accelerations are more or less constant over most of the length of the main curves of these turnouts. Such a constancy of accelerations would happen only with the smooth steering of the B-IV cars through these turnouts. For the SEPTA As-is turnout this, of course, is not so. Rapid changes in accelerations occur due to the long car adjusting to many radius of curvature changes in the turnout—an indication that the steering is not smooth. For the AREMA turnouts, these rapid changes do not occur, and both Axles 1 and 3 appear to steer the B-IV cars smoothly through these turnouts.

3.3 OTHER PARAMETERS

Figures 17 through 26 provide various plots of other parameters, such as vertical wheel loads, car body accelerations, bolster accelerations, and *L/V* ratios. The graphs in these plots are pretty much self-explanatory and reinforce the fact that the AREMA-Case 2 turnout curvature geometry is better suited for B-IV cars than that of the SEPTA As-is turnout even at low operating speeds. Only a very brief description of these parameters is given in the following sections.

3.3.1 Wheel Vertical Loads

Two factors are important when investigating wheel vertical loads: (1) magnitude of the range between loading and unloading of a wheel and the axle-to-axle variation of this range—this will indicate the ride quality as to whether the car is rocking and twisting through the turnout; and (2) the amount of unloading in comparison to the wheel static load—this is important to assess the possibility of rail roll over because of the high lateral loads exerted by a yawed axle.

Figures 17 through 19 show minimum and maximum wheel vertical loads on all axles of the B-IV car, in the facing point and trailing point runs from 5 to 25 mph, for SEPTA As-is, AREMA As-is, and AREMA-Case 2 turnouts, respectively. Also, in Table 4, the maximum unloading, loading, and the range of vertical wheel loads at 25 mph for these three turnouts are tabulated. As seen in Table 4, wheel unloading of as much as 89.5% below the wheel static load occurs at left wheel of Axle 3 in facing point run at 25 mph for the SEPTA As-is turnout. The maximum loading for this same wheel is about 67.1% above the static wheel load at 25 mph. This is a very large range. For the left wheel of Axle 1, the range is 18.3% unloading to 71.5% loading. A comparison of the maximum ranges of wheel vertical loads between leading and trailing trucks shows that the range is as much as 138% larger on the trailing truck wheels than on the leading truck wheels. This is also evident for the trailing point run.

For a facing point run at 25 mph, the AREMA As-is turnout curvature generates a maximum unloading of 100% for the wheels of the rear axle of the rear truck. As such, the

(*text continues on page 26*)

Facing Point Diverging Right, Point of Switch = 156 ft Lateral Accelerations of Axles 1 & 3

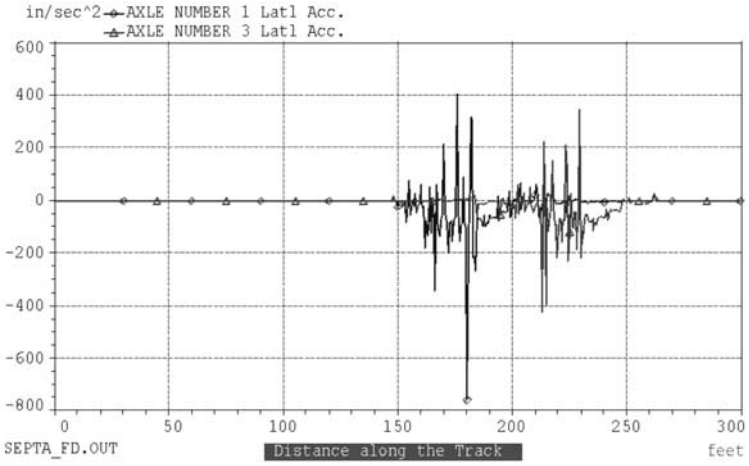

Trailing Point Diverging Left, Point of Switch = 144 ft Lateral Accelerations of Axles 1 & 3

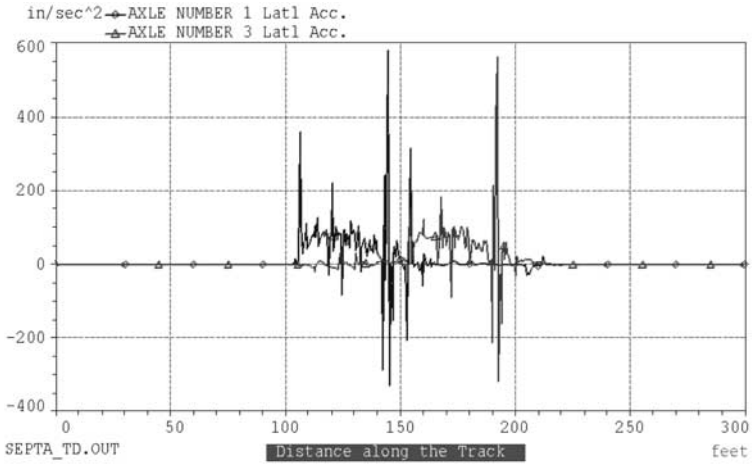

Facing Point Diverging Right, Point of Switch = 156 ft Yaw Accelerations of Axles 1 & 3

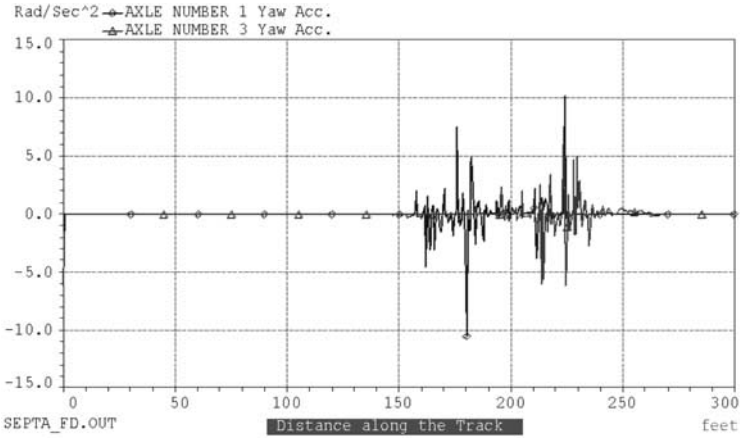

Trailing Point Diverging Left, Point of Switch = 144 ft Yaw Accelerations of Axles 1 & 3

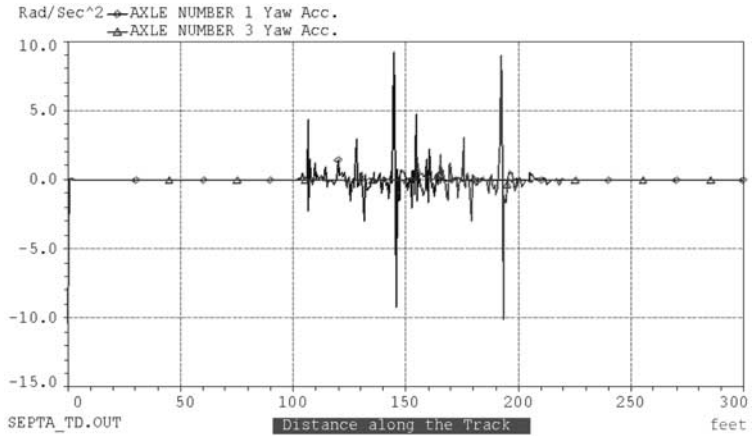

Figure 11. Lateral and yaw accelerations of axles 1 and 3 for "SEPTA As-is" turnouts at 25 mph.

Facing Point Diverging Right, Point of Switch = 156 ft Lateral Accelerations of Axles 1 & 3

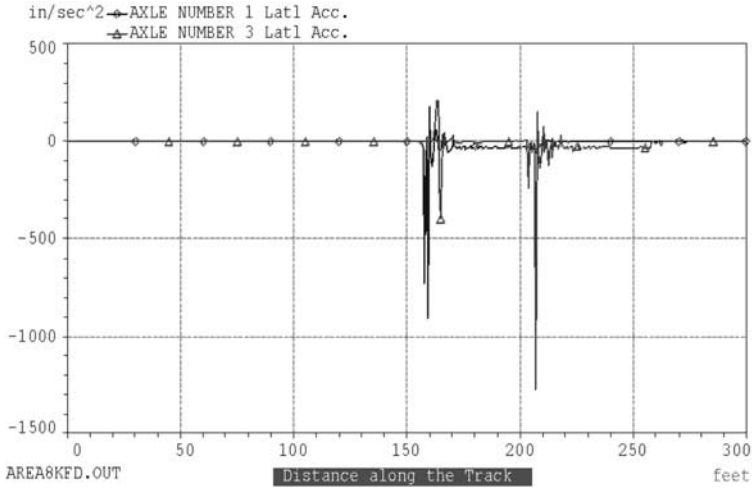

Trailing Point Diverging Left, Point of Switch = 144 ft Lateral Accelerations of Axles 1 & 3

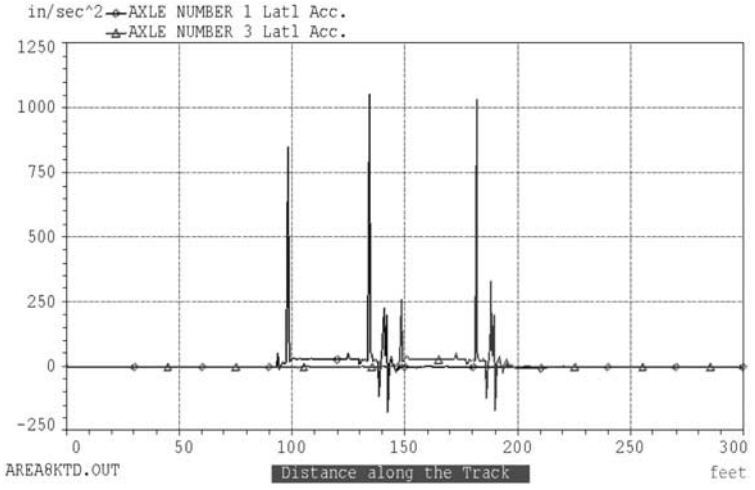

Facing Point Diverging Right, Point of Switch = 156 ft Yaw Accelerations of Axles 1 & 3

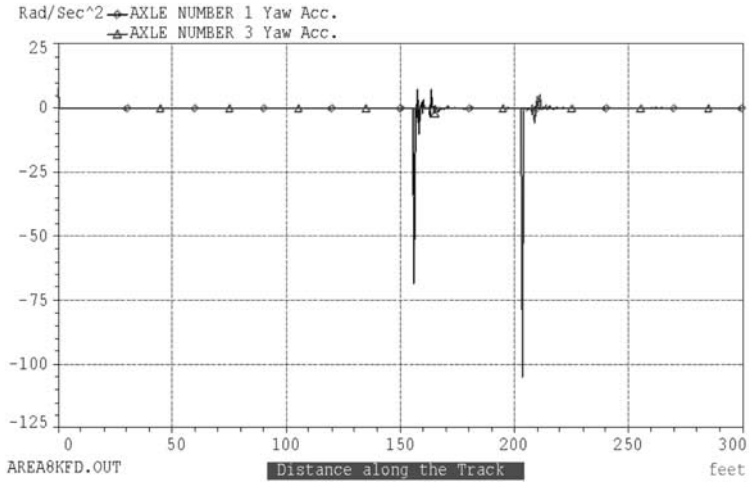

Trailing Point Diverging Left, Point of Switch = 144 ft Yaw Accelerations of Axles 1 & 3

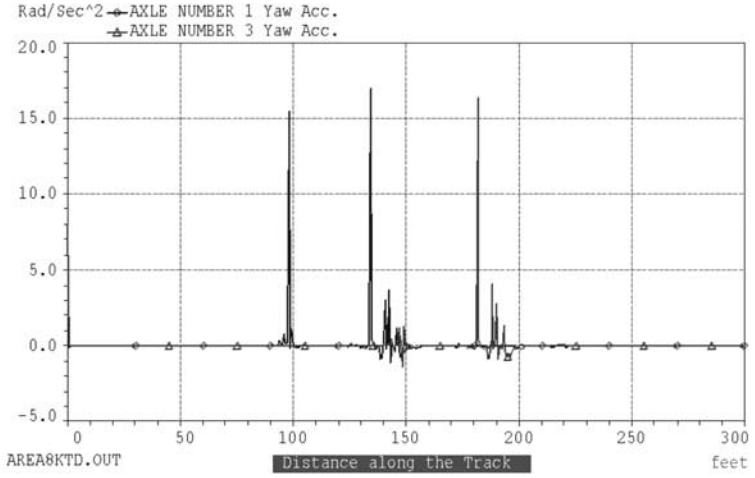

Figure 12. Lateral and yaw accelerations of axles 1 and 3 for AREMA As-is turnouts at 25 mph.

Facing Point Diverging Right, Point of Switch = 156 ft Lateral Accelerations of Axles 1 & 3

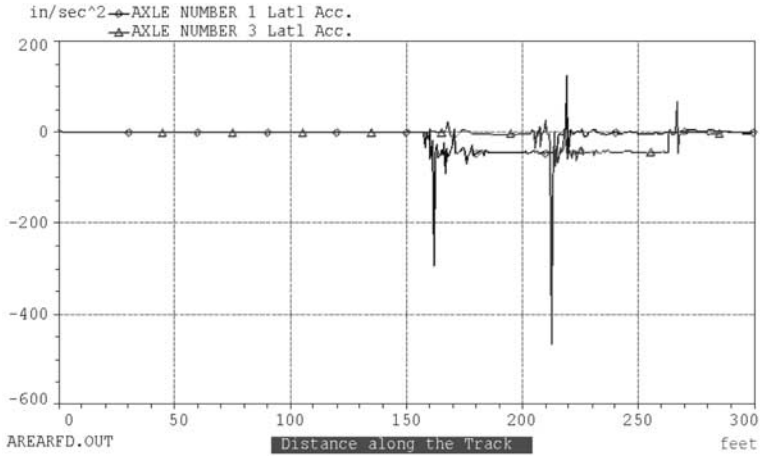

Trailing Point Diverging Left, Point of Switch = 144 ft Lateral Accelerations of Axles 1 & 3

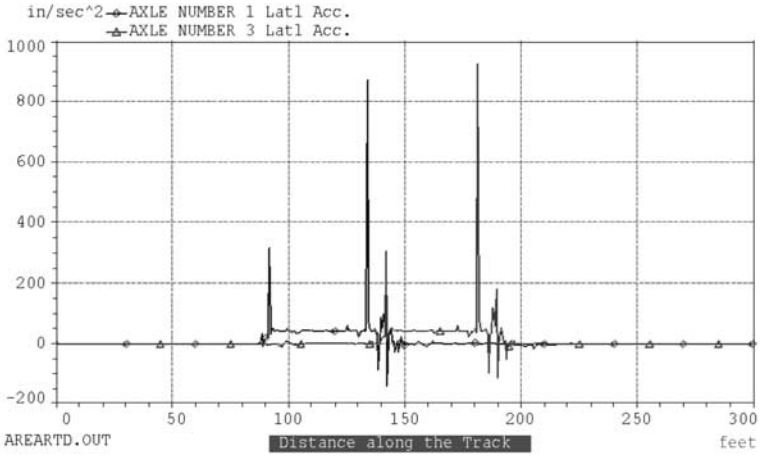

Facing Point Diverging Right, Point of Switch = 156 ft Yaw Accelerations of Axles 1 & 3

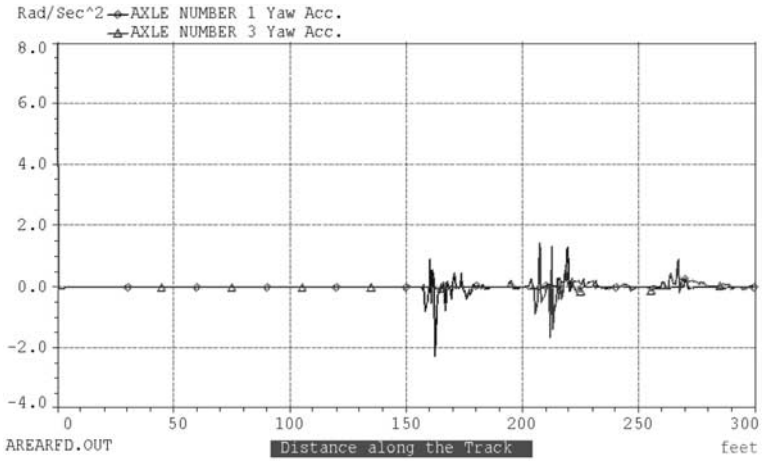

Trailing Point Diverging Left, Point of Switch = 144 ft Yaw Accelerations of Axles 1 & 3

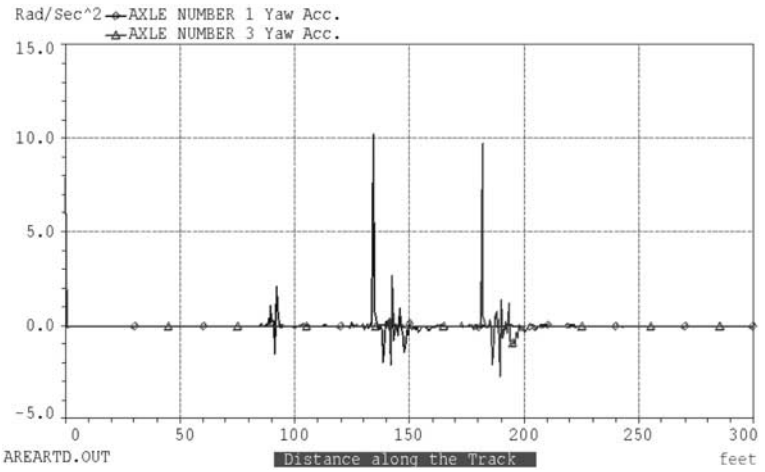

Figure 13. Lateral and yaw accelerations of axles 1 and 3 for AREMA-Case 2 turnouts at 25 mph.

Facing Point Diverging Right, Point of Switch = 156 ft Lateral Accelerations of Axles 1 & 3

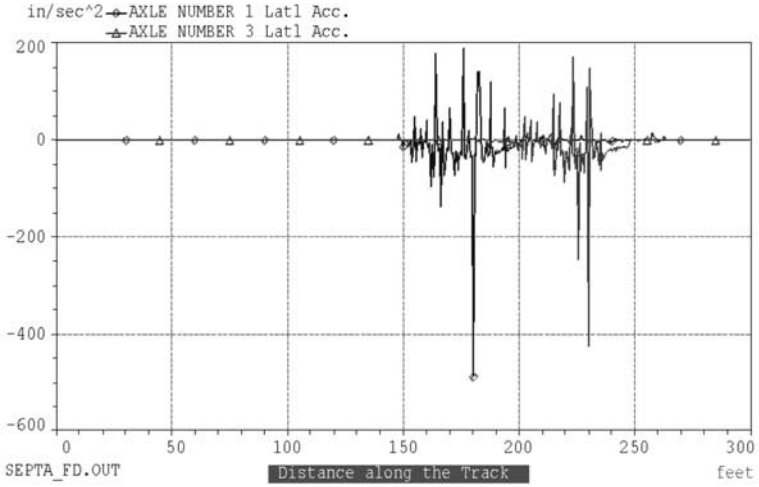

Trailing Point Diverging Left, Point of Switch = 144 ft Lateral Accelerations of Axles 1 & 3

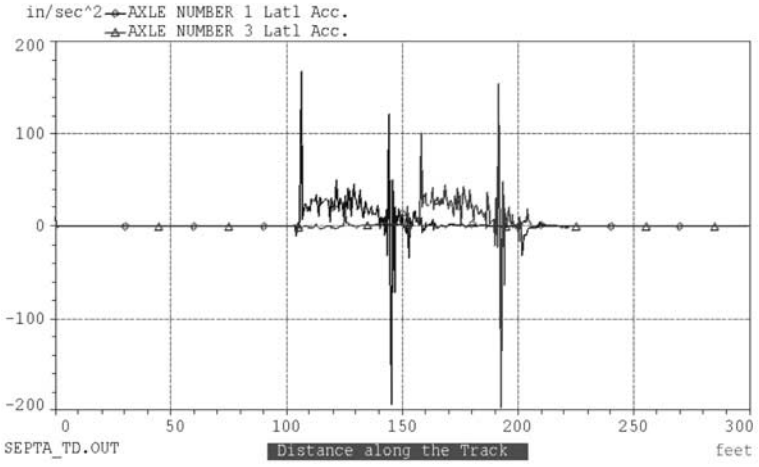

Facing Point Diverging Right, Point of Switch = 156 ft Yaw Accelerations of Axles 1 & 3

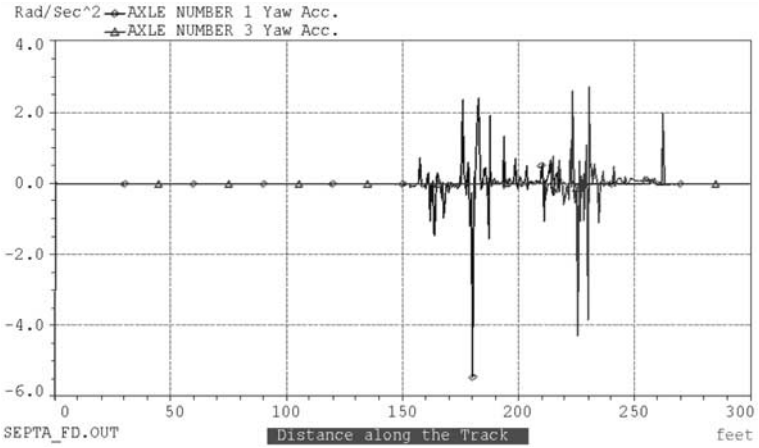

Trailing Point Diverging Left, Point of Switch = 144 ft Yaw Accelerations of Axles 1 & 3

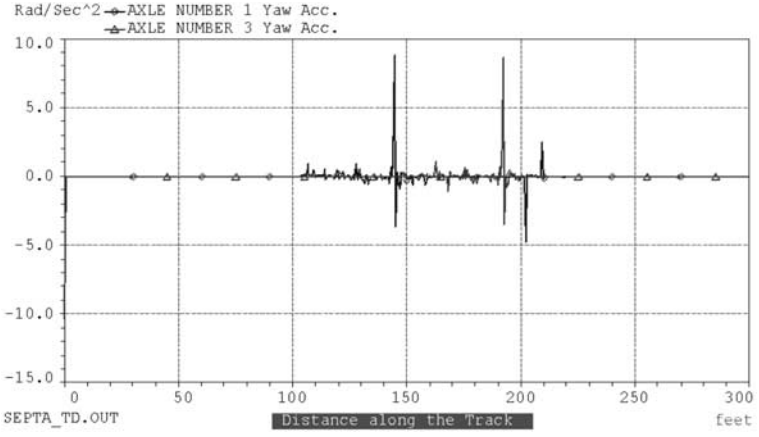

Figure 14. Lateral and yaw accelerations of axles 1 and 3 for "SEPTA As-is" turnouts at 15 mph.

Facing Point Diverging Right, Point of Switch = 156 ft Lateral Accelerations of Axles 1 & 3

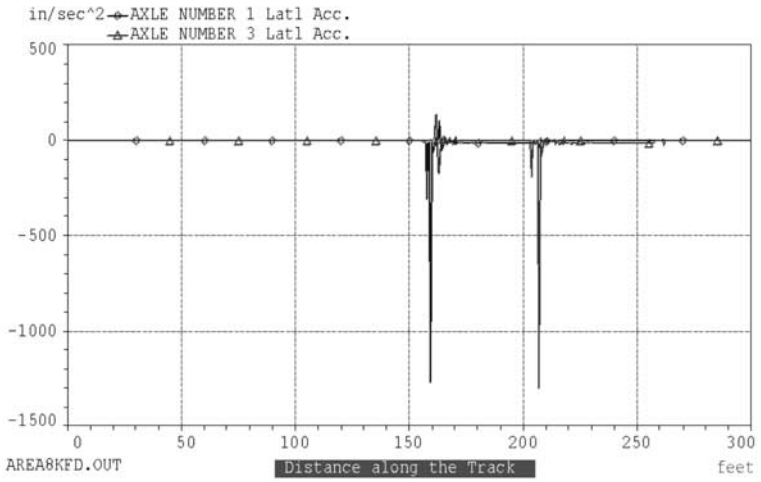

Trailing Point Diverging Left, Point of Switch = 144 ft Lateral Accelerations of Axles 1 & 3

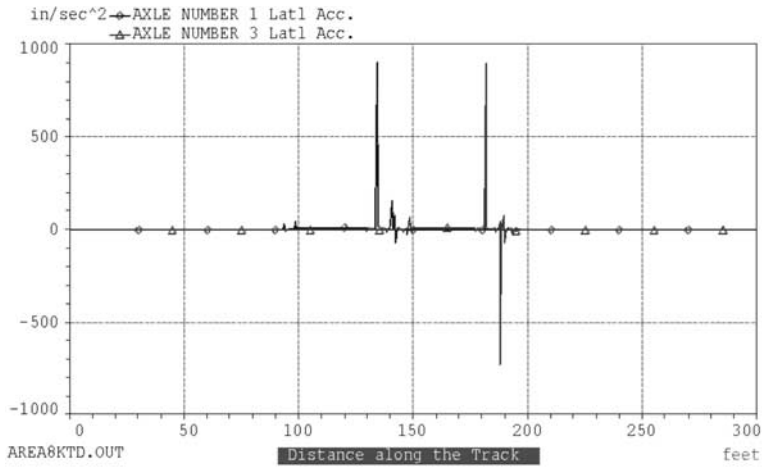

Facing Point Diverging Right, Point of Switch = 156 ft Yaw Accelerations of Axles 1 & 3

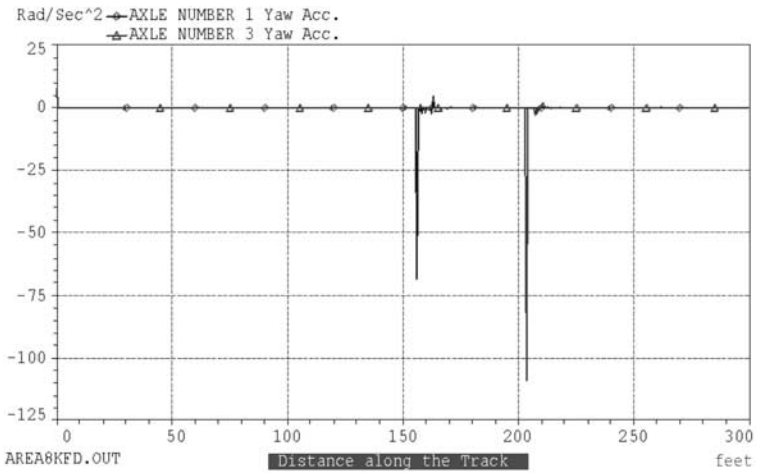

Trailing Point Diverging Left, Point of Switch = 144 ft Yaw Accelerations of Axles 1 & 3

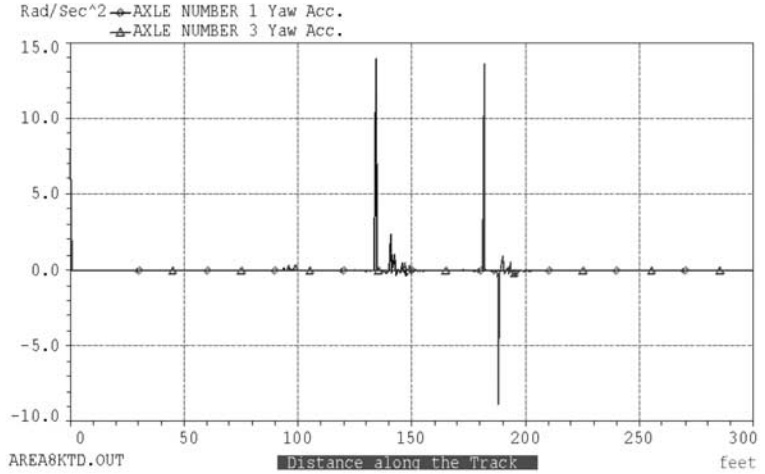

Figure 15. Lateral and yaw accelerations of axles 1 and 3 for AREMA As-is turnouts at 15 mph.

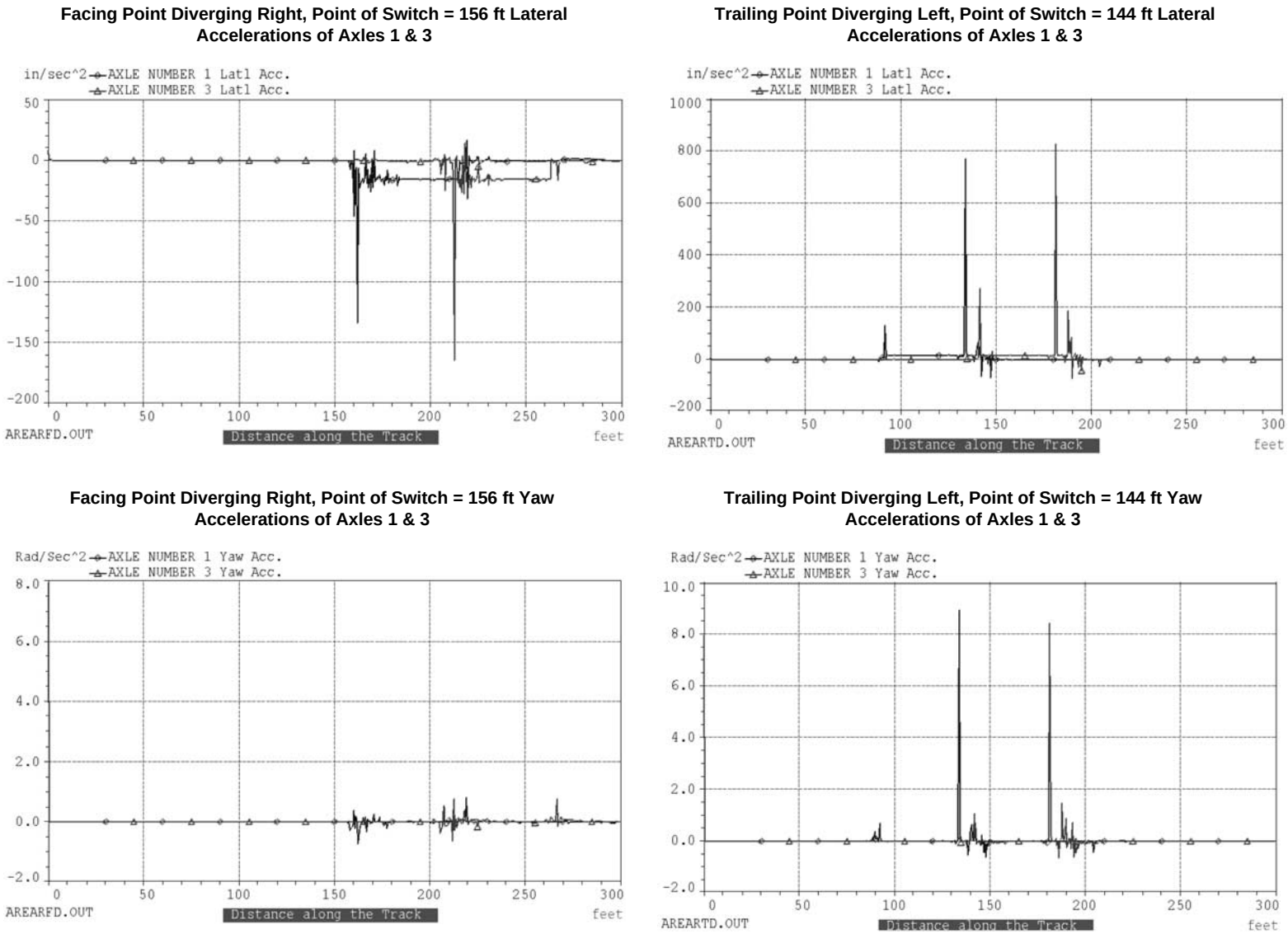

Figure 16. Lateral and yaw accelerations of axles 1 and 3 for AREMA-Case 2 turnouts at 15 mph.

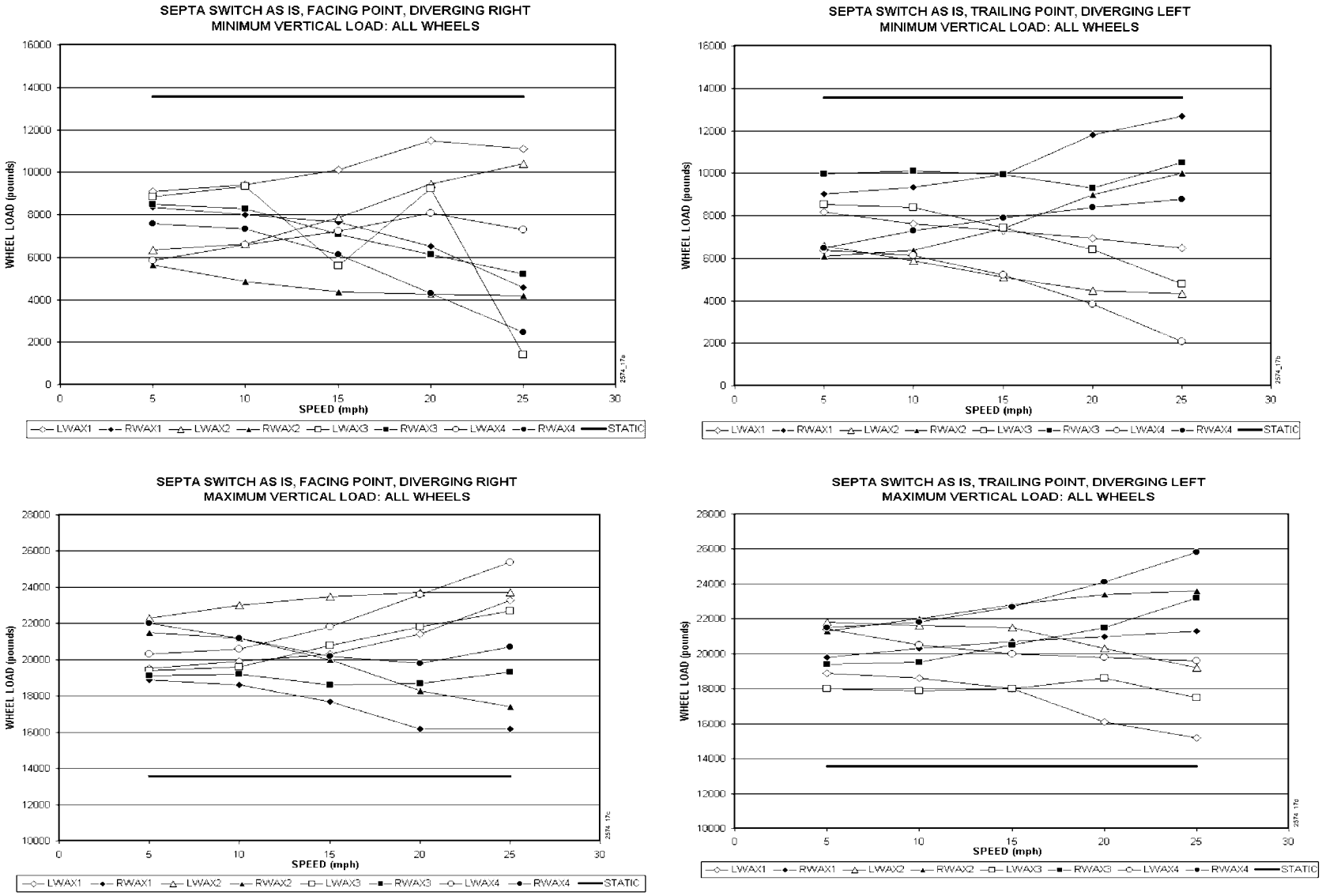

Figure 17. Minimum and maximum vertical wheel loads for SEPTA As-is turnout for speeds from 5 to 25 mph.

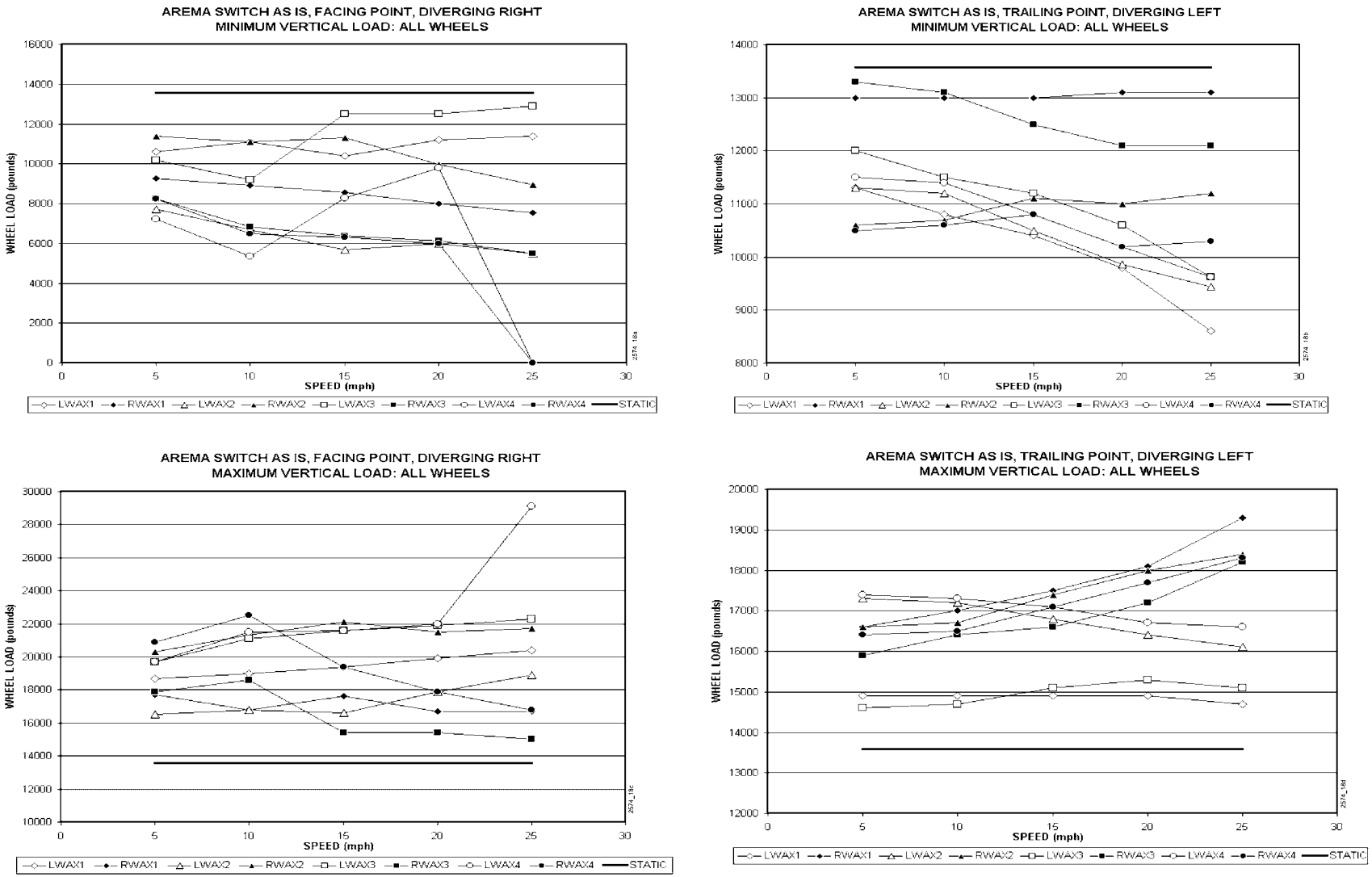

Figure 18. Minimum and maximum vertical wheel loads for AREMA As-is turnout for speeds from 5 to 25 mph.

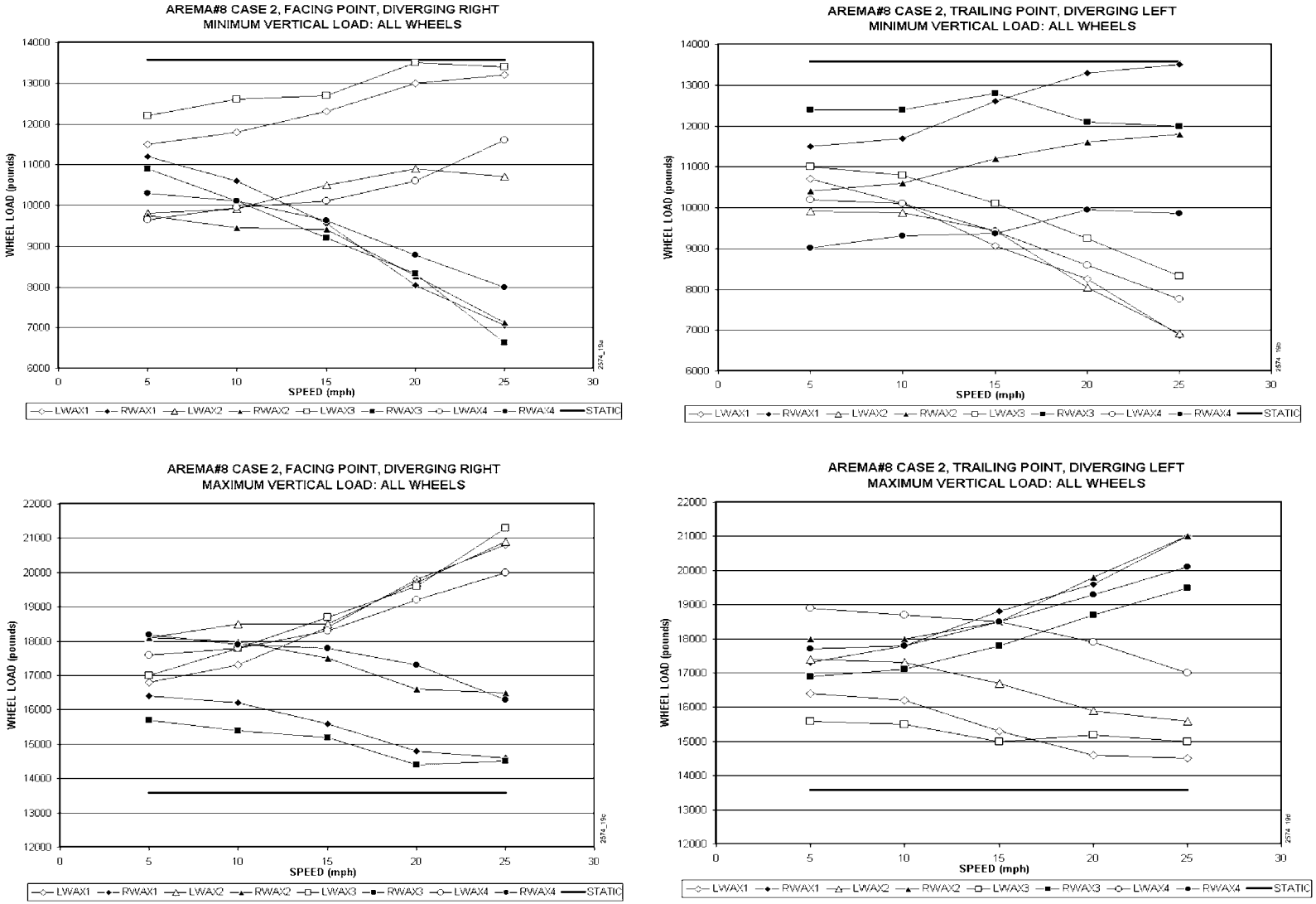

Figure 19. Minimum and maximum vertical wheel loads for AREMA-Case 2 turnout for speeds from 5 to 25 mph.

TABLE 4 Maximum unloading, loading and range of vertical wheel loads for SEPTA As-is, AREMA As-is, and AREMA-Case 2 turnouts at 25 mph

Facing Point Run		SEPTA As-is			AREMA As-is			AREMA-Case 2		
25 mph		Max (%)	Max (%)	Max (%)	Max (%)	Max (%)	Max (%)	Max (%)	Max (%)	Max (%)
Wheel	Axle	Unloading	Loading	Range	Unloading	Loading	Range	Unloading	Loading	Range
Left	1	18.3	71.5	89.8	16.1	50.2	66.3	2.8	53.1	55.9
Right	1	66.2	19.3	85.5	44.4	23.7	68.1	48.1	7.5	55.6
Left	2	23.4	74.5	97.9	59.6	39.1	98.7	21.2	53.9	75.1
Right	2	69.1	28.1	97.2	34.2	59.8	94.0	47.6	21.5	69.1
Left	3	89.5	67.1	156.6	5.0	64.2	69.2	1.3	56.8	58.1
Right	3	61.7	42.1	103.8	59.6	10.4	70.0	51.2	6.8	58.0
Left	4	46.3	87.0	133.3	100.0	114.2	214.2	14.6	47.2	61.8
Right	4	81.8	52.4	134.2	100.0	23.7	123.7	41.2	20.0	61.2
Trailing Point										
25 mph										
Wheel	Axle									
Left	1	52.3	11.9	64.2	36.6	8.2	44.8	49.0	6.8	55.8
Right	1	6.5	56.8	63.3	3.6	42.1	45.7	0.6	54.6	55.2
Left	2	68.0	41.4	109.4	30.5	18.5	49.0	49.0	14.8	63.8
Right	2	26.4	73.7	100.1	17.5	35.5	53.0	13.1	54.6	67.7
Left	3	64.8	28.8	93.6	29.2	11.2	40.4	38.7	10.4	49.1
Right	3	22.7	70.8	93.5	10.9	34.0	44.9	11.7	43.6	55.3
Left	4	84.6	44.3	128.9	29.2	22.2	51.4	42.8	25.1	67.9
Right	4	35.3	89.9	125.2	24.2	34.7	58.9	27.4	48.0	75.4

maximum ranges on these wheels are quite large. A check of the history of the 25-mph run, however, showed that Axle 4 at the time of 100% unloading was still on the tangent track before the point of switch, the axle was almost radial, and that the lateral load was zero at this instant. In the trailing point run at 25 mph through this turnout, the maximum unloading, loading, and range of vertical loads on all wheels are quite small however.

In contrast, for the AREMA-Case 2 turnout at 25 mph, the maximum unloading, loading, and range of vertical loads on all wheels are quite small for both the facing point and trailing point runs. These much smaller ranges between vertical loading and unloading of the B-IV car wheels for the AREMA-Case 2 turnout only indicate a much improved ride quality over that of the SEPTA As-is turnout.

3.3.2 Car Body and Bolster Accelerations

Figures 20 and 21 shows the most negative and most positive car body lateral and yaw accelerations at speeds from 5 to 25 mph. Figure 22 shows the most negative and positive lateral accelerations for the leading bolster. A comparison of car body lateral accelerations shows that the B-IV car body has less acceleration through the curvature of AREMA-Case 2 turnout than the SEPTA As-is turnout over all of the speeds from 5 to 25 mph. In fact, this acceleration response of the car body improves comparatively for the AREMA-Case 2 turnout at higher speeds. Car body yaw accelerations also show a similar trend. Bolster lateral accelerations are quite close to each other for the AREMA-Case 2 and SEPTA As-is turnouts in the facing point runs. In the trailing point runs, bolster accelerations in AREMA-Case 2 turnout are quite low as compared with the SEPTA As-is turnout. Again, there is a comparative improvement for AREMA-Case 2 turnout at higher speeds in the trailing point runs.

A better ride quality through the AREMA-Case 2 turnout is therefore indicated by the smaller car body lateral and yaw accelerations, as shown in Figures 20 and 21, and smaller bolster lateral accelerations, shown in Figure 22.

3.3.3 Wheel and Axle L/V Ratios

Figures 23, 24, and 25 show the most negative and most positive wheel L/V ratios for SEPTA As-is, AREMA As-is, and AREMA-Case 2 turnouts, respectively, for speeds from 5 to 25 mph. Axle sum L/V ratios for these turnouts are given in Figure 26.

The attacking, or steering, axles are the first and third axles. For the facing-point diverging-right runs, the most important wheel is the left wheel of Axle 1; and for the trailing-point diverging-left runs, it is the right wheel of Axle 1. As seen in Figure 23, the corresponding maximum L/V ratios on these wheels are –0.757 at 25 mph in the facing point run, and from 1.06 to 1.08 between 15 and 25 mph in the trailing point runs through the SEPTA As-is turnout. The same for AREMA As-is turnout are –1.02 and 0.963, both at 25 mph (Figure 24). In Figure 25, these values for the AREMA-Case 2 turnout are –0.694 for left wheel of Axle 1 and 0.944 for the right wheel of Axle 1, respectively, for the facing point and trailing point

(*text continues on page 37*)

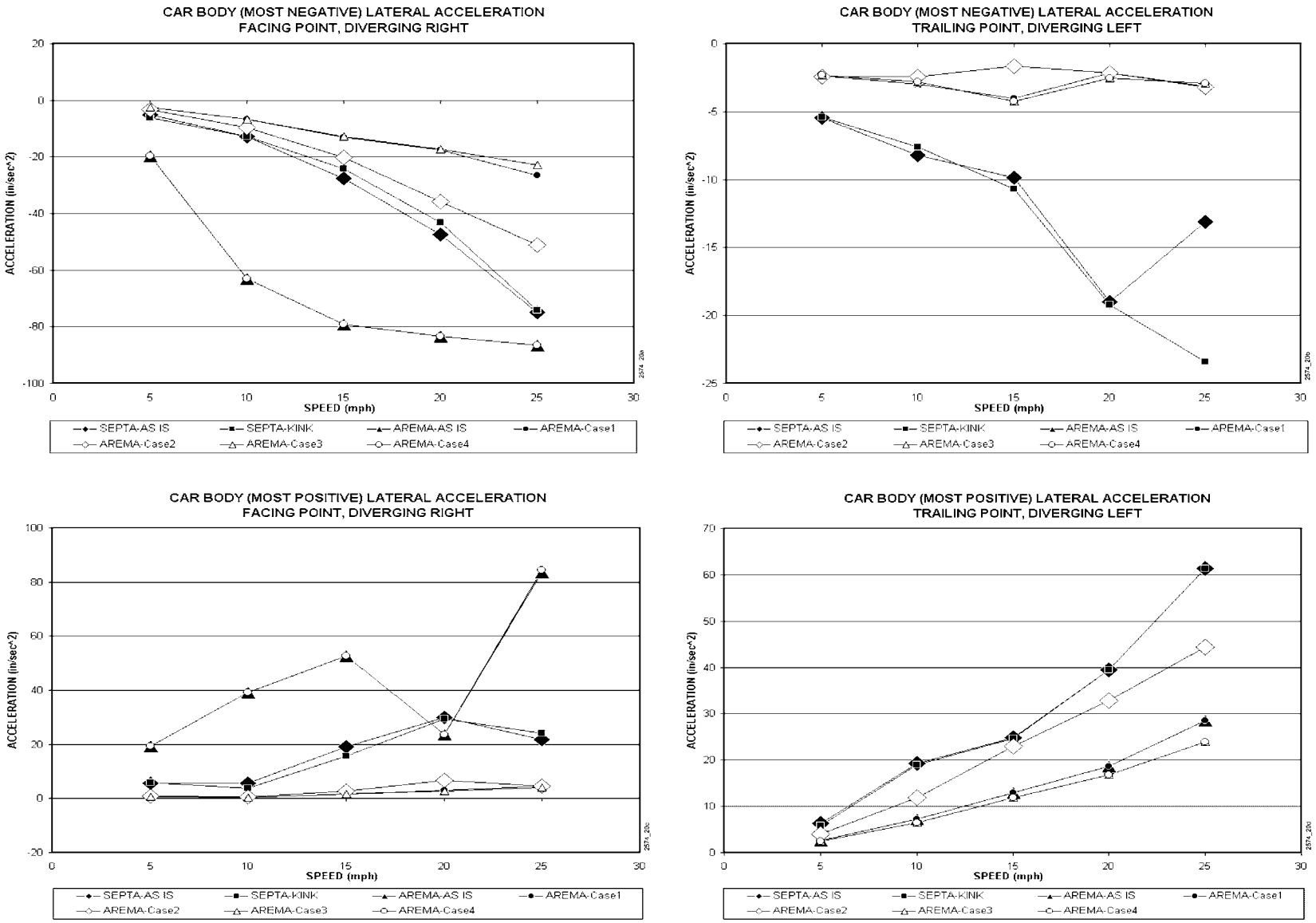

Figure 20. Most negative and most positive car body lateral accelerations in facing point and trailing point runs for speeds from 5 to 25 mph.

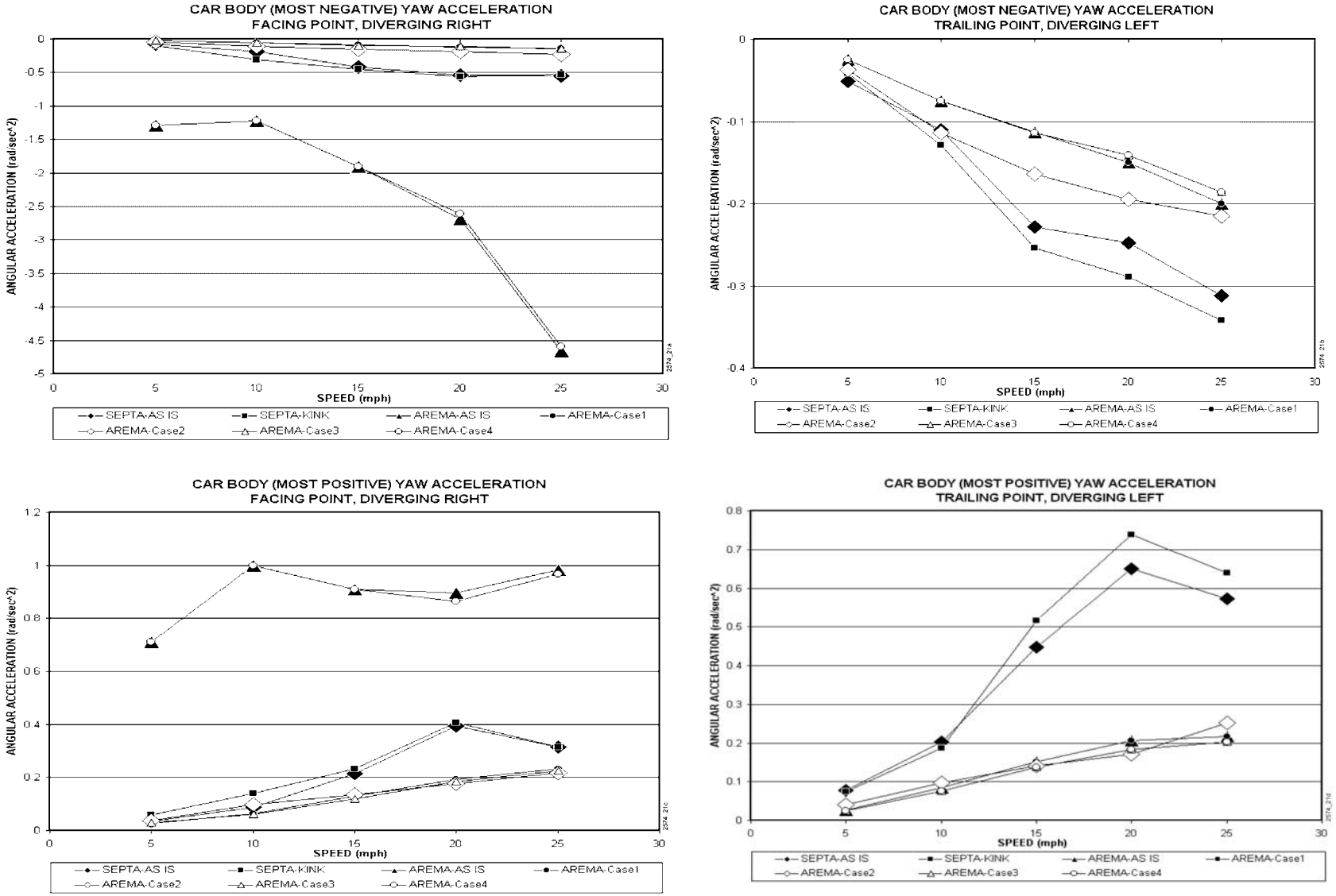

Figure 21. Most negative and most positive car body yaw accelerations in facing point and trailing point runs for speeds from 5 to 25 mph.

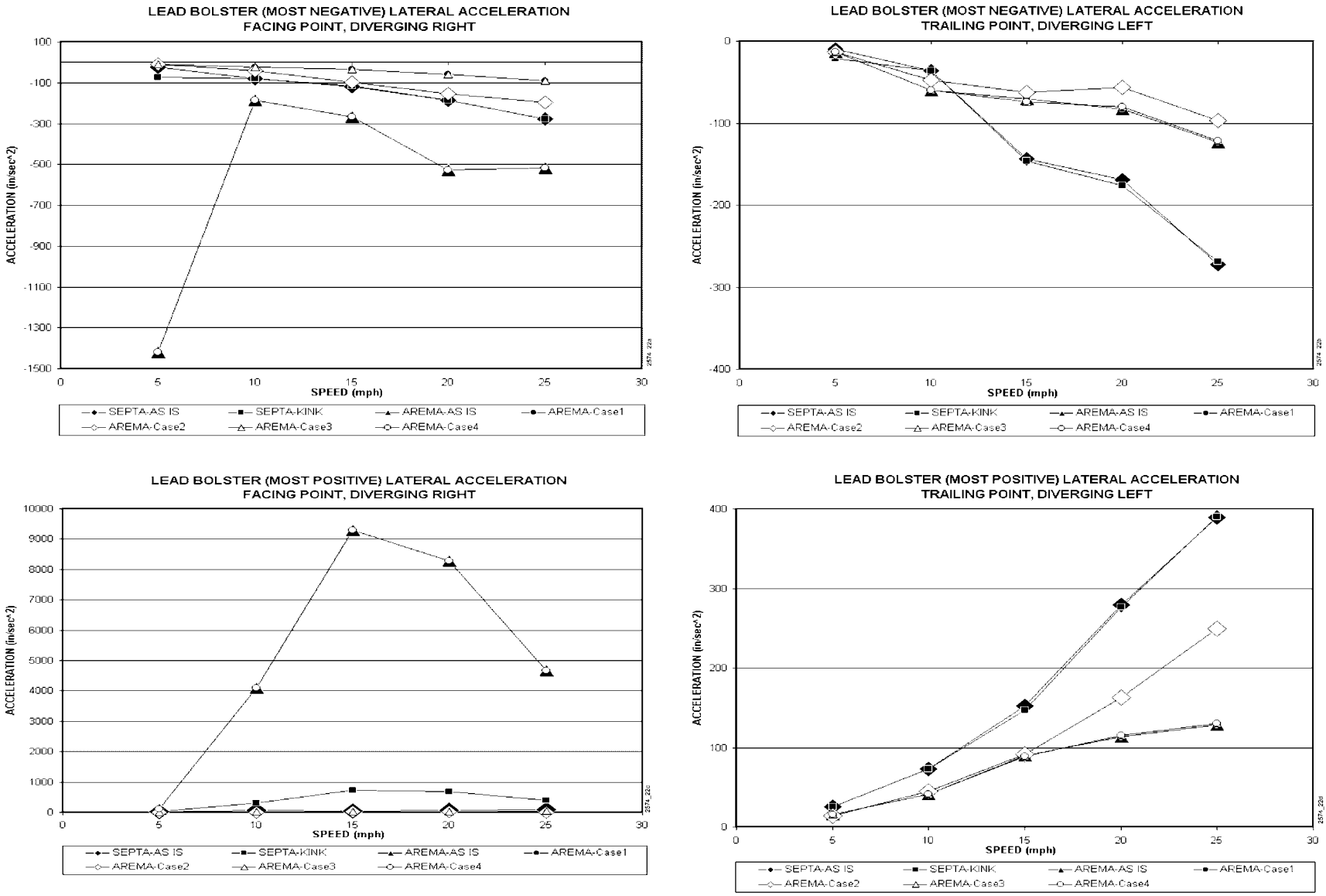

Figure 22. Most negative and most positive lead bolster lateral accelerations in facing point and trailing point runs for speeds from 5 to 25 mph.

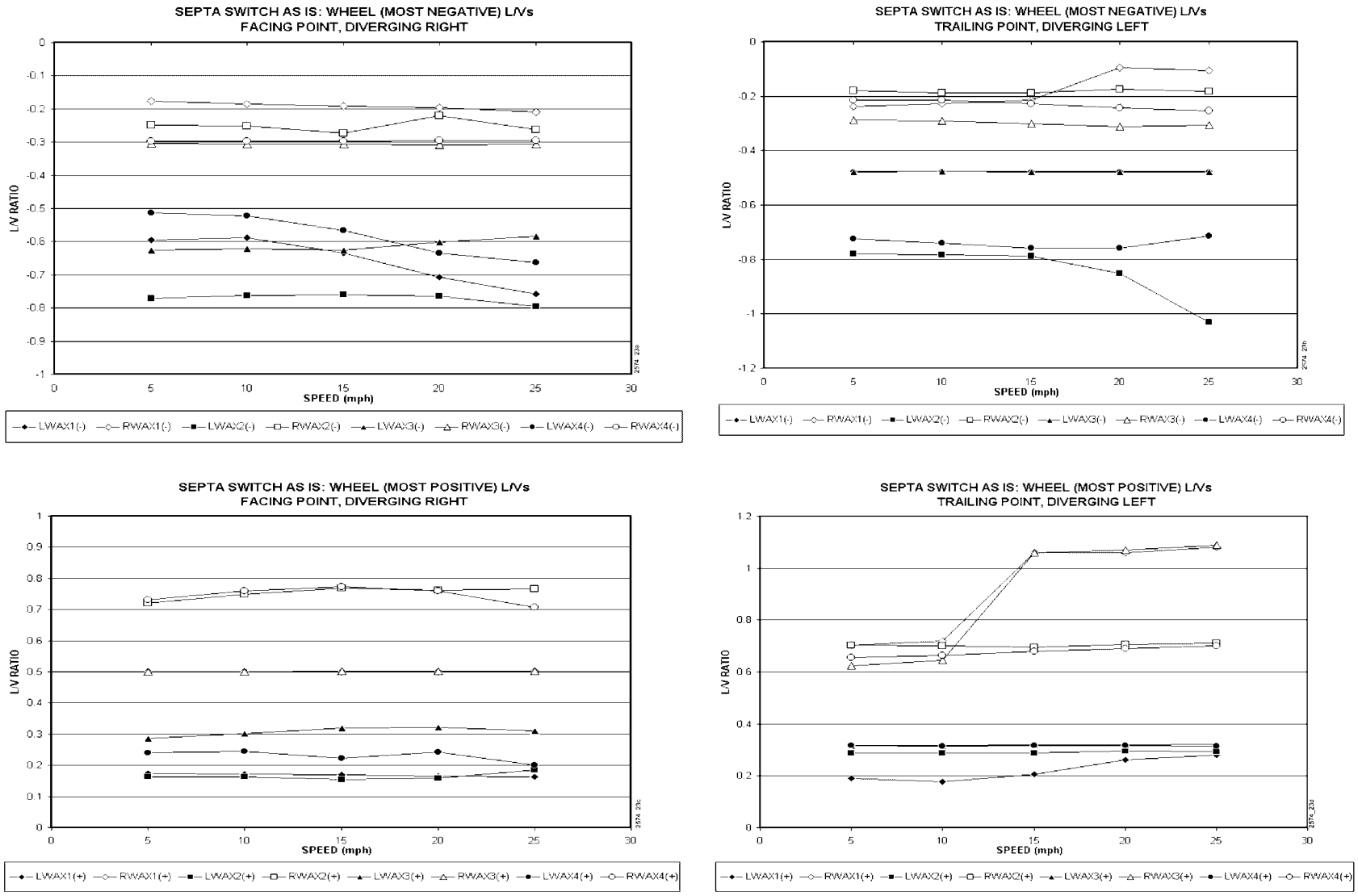

Figure 23. Most negative and most positive wheel L/V ratios for SEPTA As-is turnout for speeds from 5 to 25 mph.

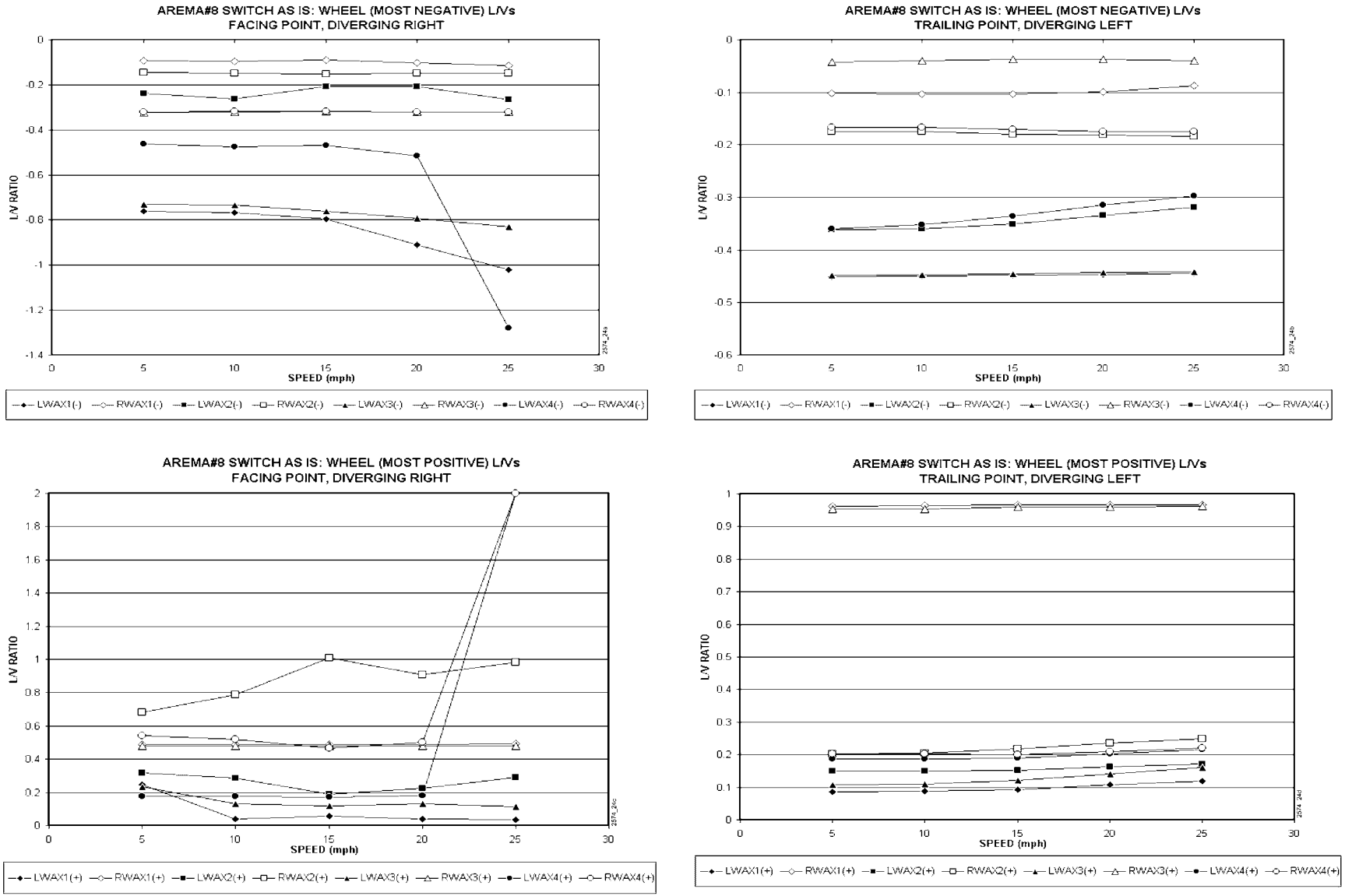

Figure 24. Most negative and most positive wheel L/V ratios for AREMA As-is turnout for speeds from 5 to 25 mph.

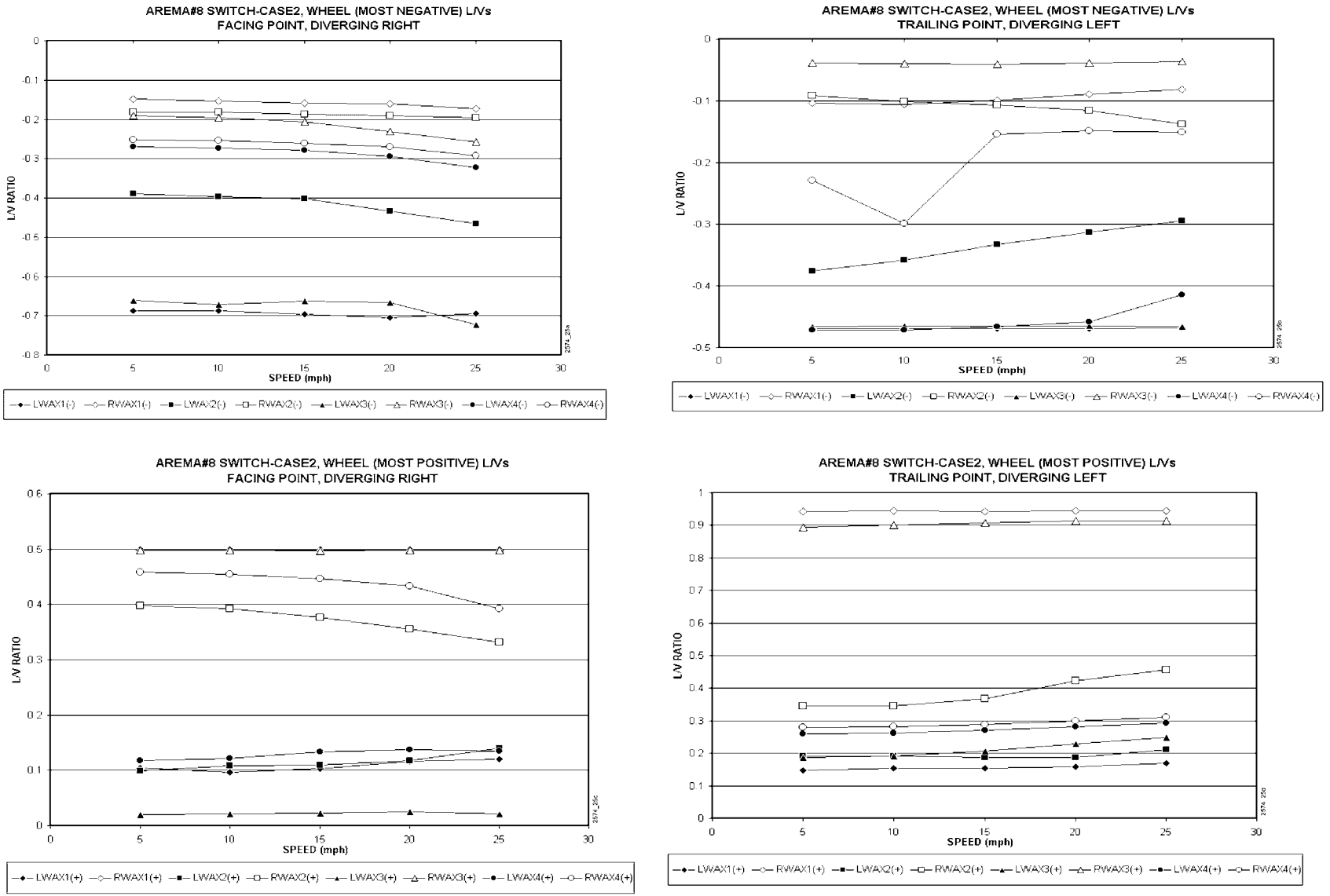

Figure 25. Most negative and most positive wheel L/V ratios for AREMA-Case 2 turnout for speeds from 5 to 25 mph.

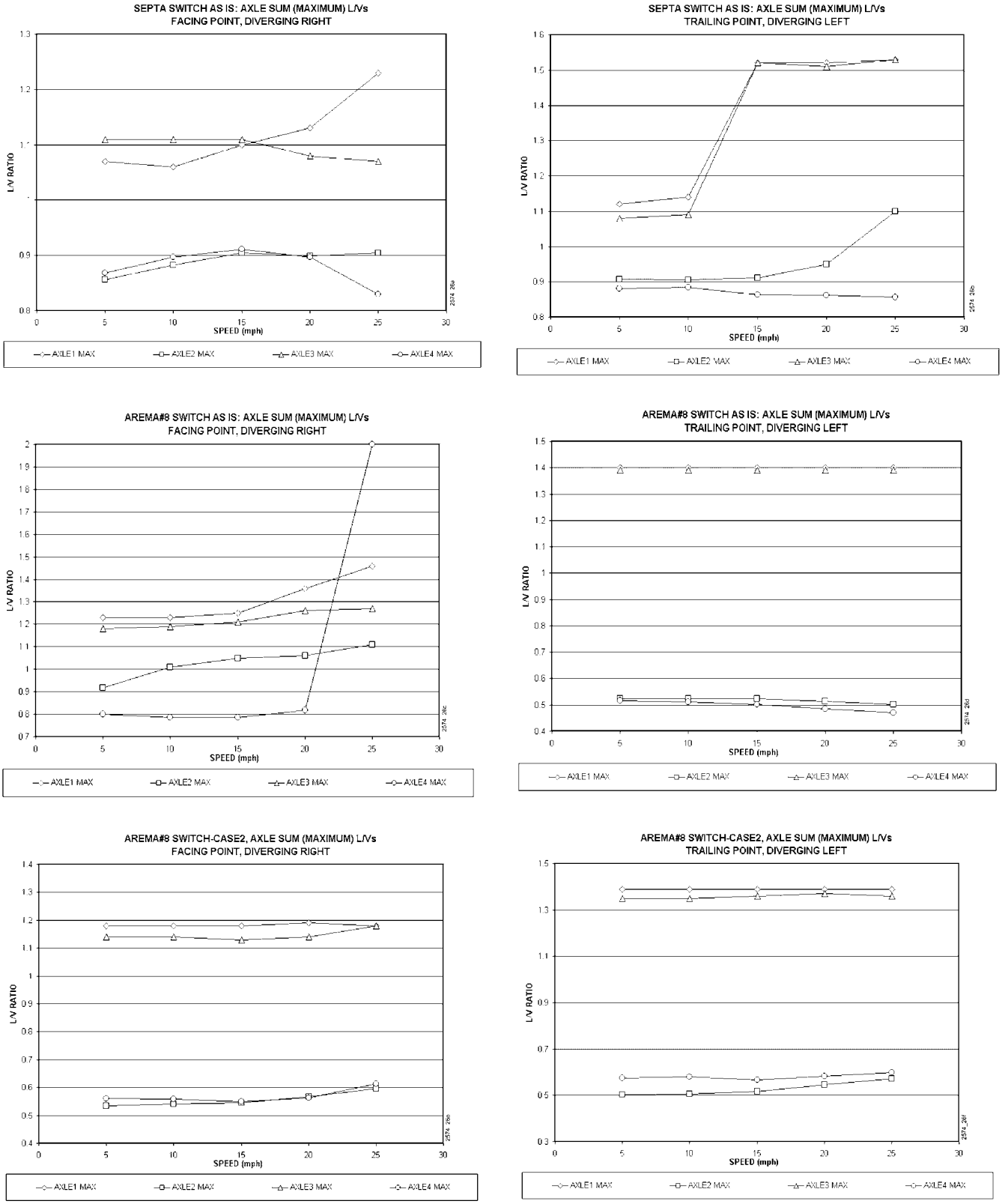

Figure 26. Comparison of axle sum L/V ratios between SEPTA As-is, AREMA As-is, and AREMA-Case 2 turnouts for speeds from 5 to 25 mph.

Facing Point Diverging Right, Left Wheel

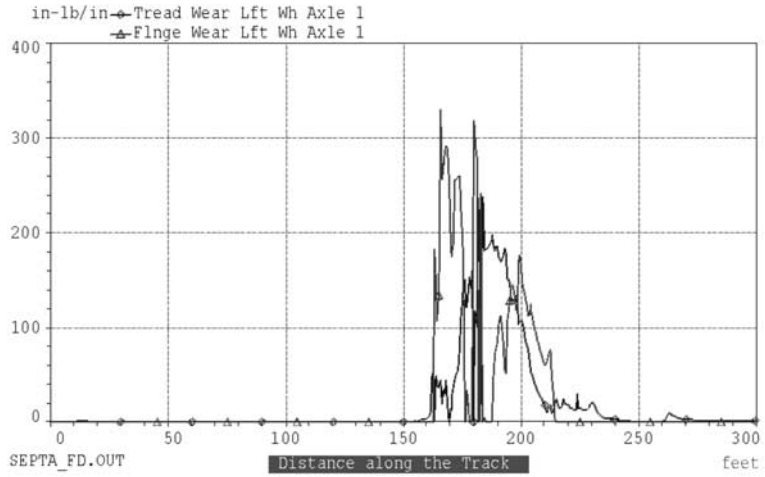

Facing Point Diverging Right, Right Wheel

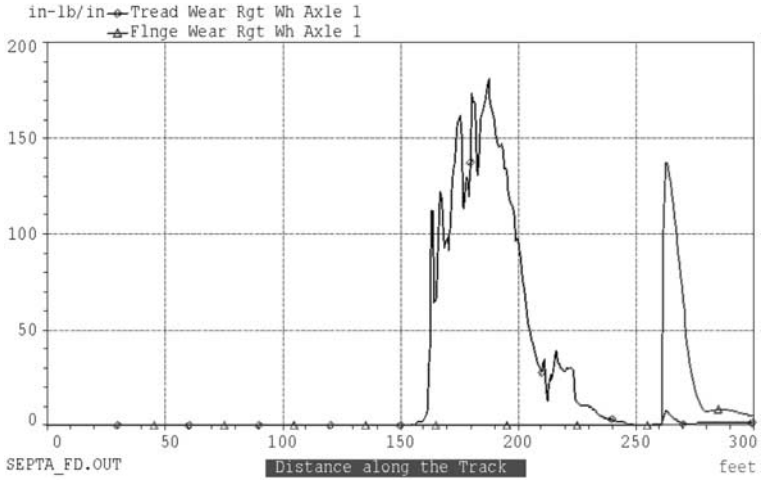

Trailing Point Diverging Left, Left Wheel

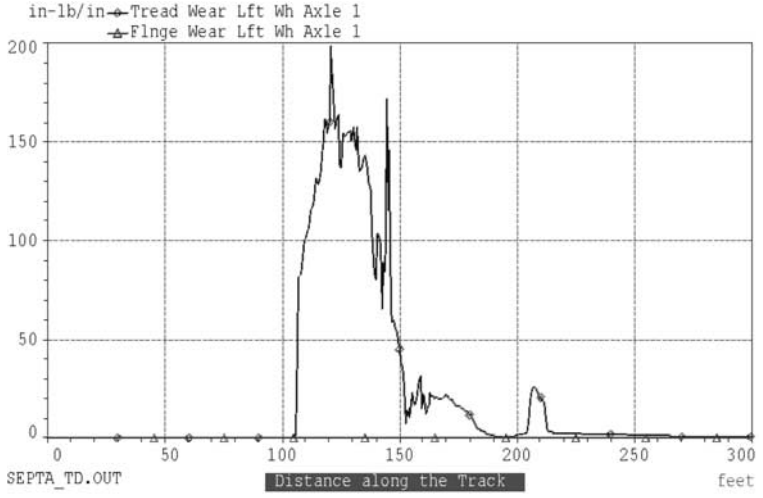

Trailing Point Diverging Left, Right Wheel

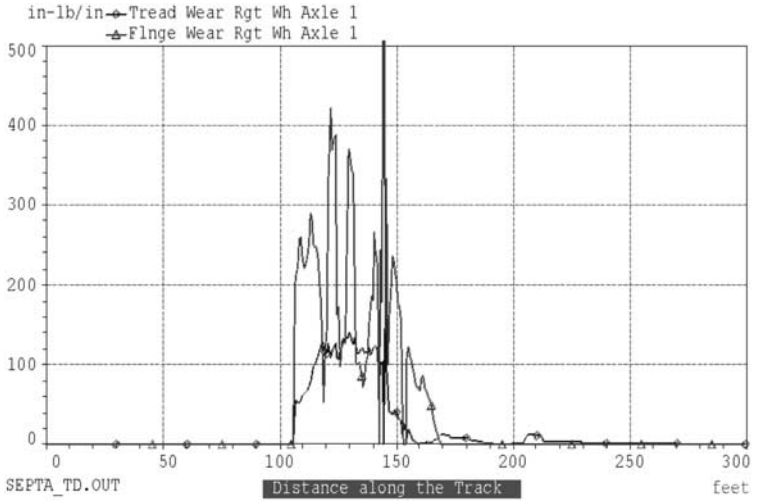

Figure 27. Tread and flange wear indices of axle 1 wheels at 25 mph for the SEPTA As-is turnout.

Facing Point Diverging Right, Left Wheel

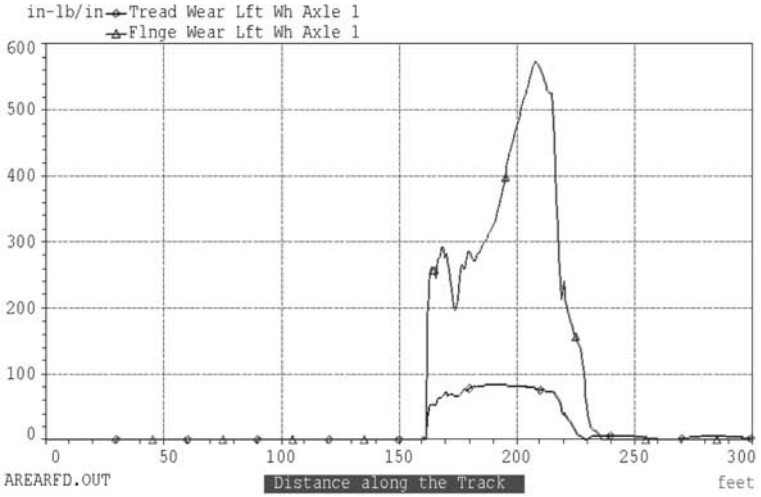

Facing Point Diverging Right, Right Wheel

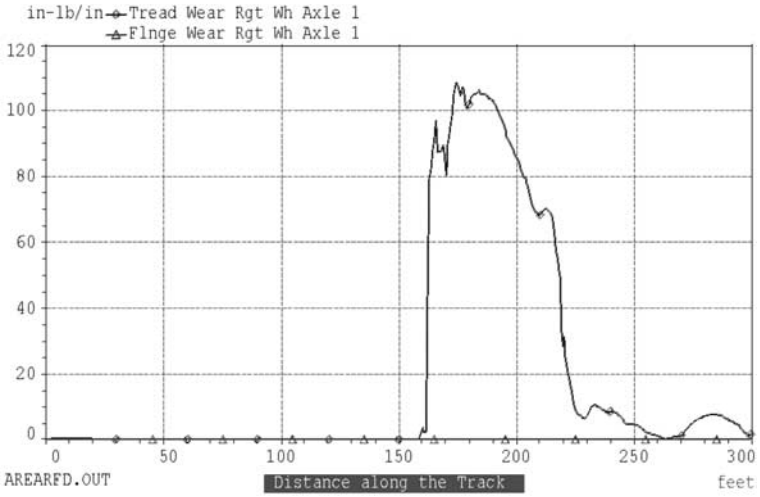

Trailing Point Diverging Left, Left Wheel

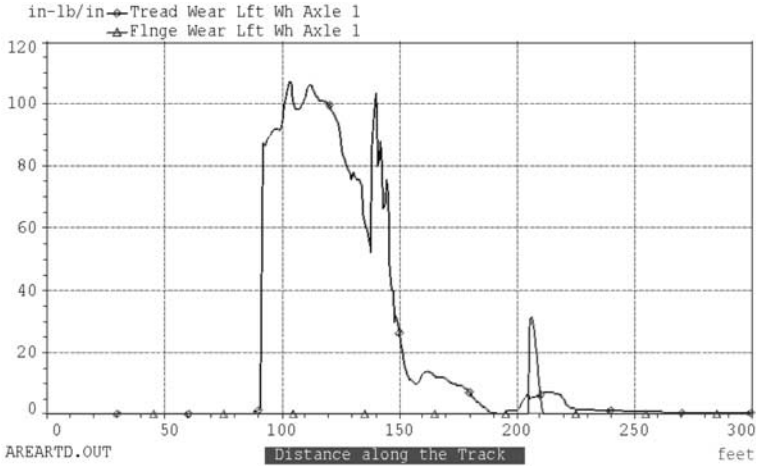

Trailing Point Diverging Left, Right Wheel

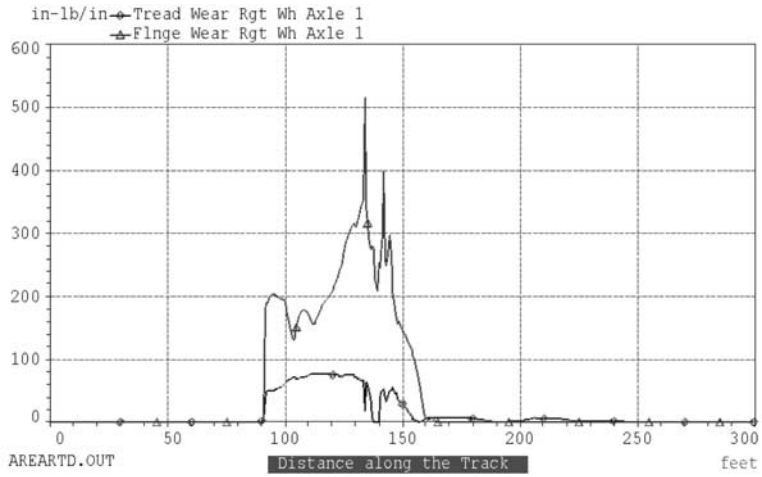

Figure 28. Tread and flange wear indices of axle 1 wheels at 25 mph for AREMA-Case 2 turnout.

Facing Point Diverging Right, Left Wheel

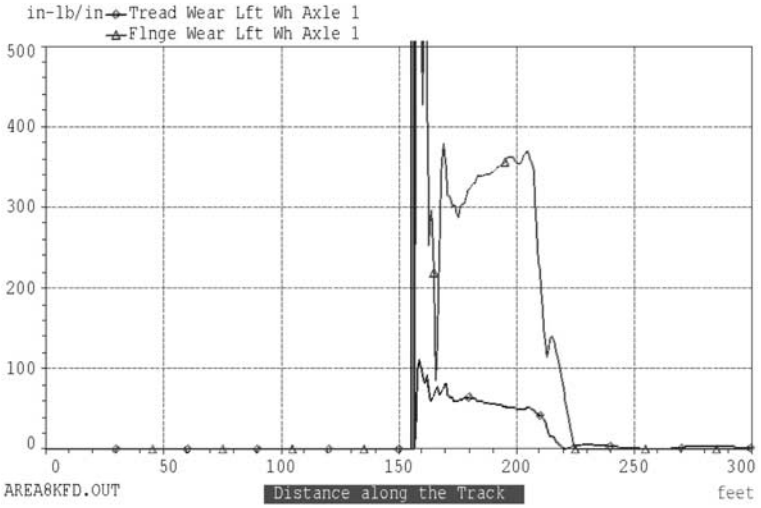

Facing Point Diverging Right, Right Wheel

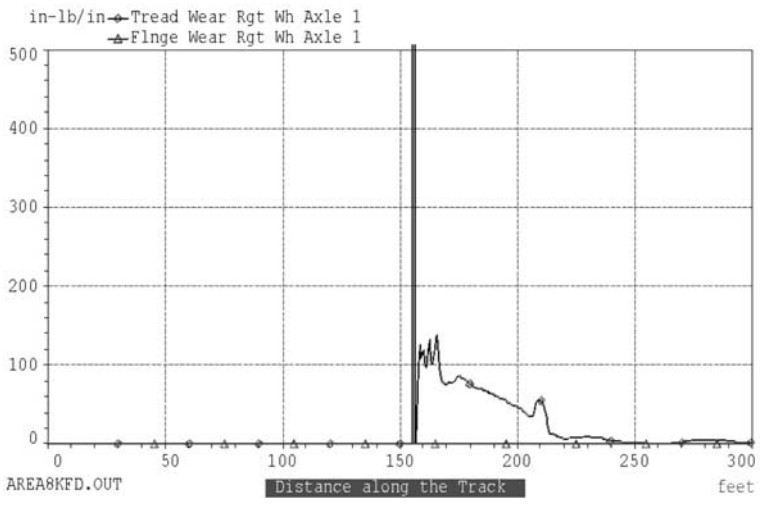

Trailing Point Diverging Left, Left Wheel

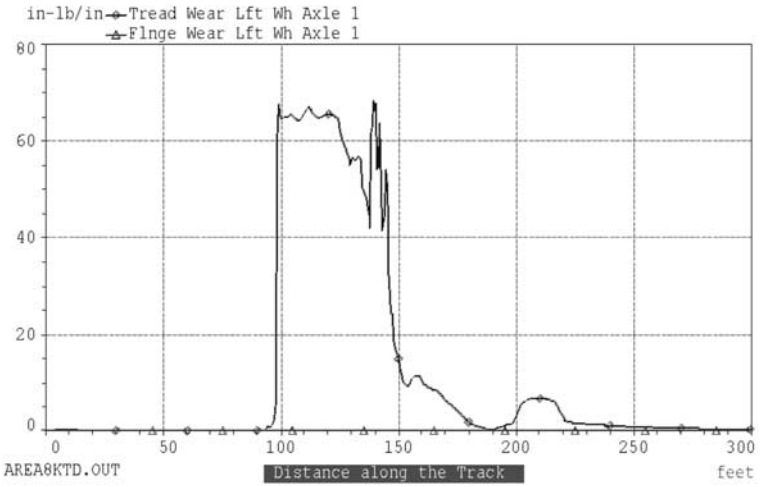

Trailing Point Diverging Left, Right Wheel

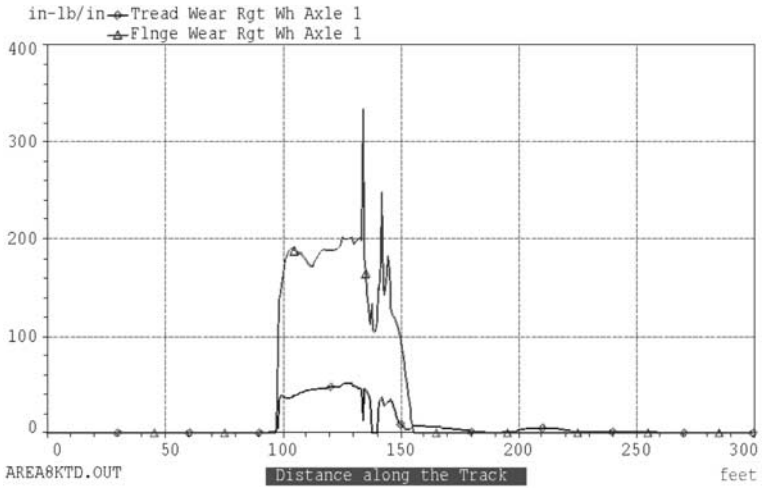

Figure 29. Tread and flange wear indices of axle 1 wheels at 25 mph for AREMA As-is turnout.

runs. Again, the negative results are due to the lateral load sign convention used in the NUCARS™ program.

Given that the increase in vertical wheel loading is higher in the SEPTA As-is turnout, the *L*/*V* ratios have greater significance in this turnout than in the AREMA-Case 2 turnout. Correspondingly, rail rollover is more of a possibility for the SEPTA As-is turnout than the AREMA-Case 2 turnout. Also, the possibility of wheel climb derailment, as indicated by a greater wheel *L*/*V* ratio than the threshold value of 1.0 of the Nadal criterion *(8)* (dry wheel and rail conditions), should not be overlooked for the SEPTA As-is turnout for speeds from 15 to 25 mph in the trailing point runs or for the AREMA As-is turnout at 25 mph in the facing point run.

Given that wheels are not independently attached to the car body, the effect of the connection by the axle of the two wheels is given as axle sum *L*/*V* ratios (Figure 26). The effect on gage spreading by the wheels of the yawed axle is generally gauged by this parameter. As can be seen in the graphs in Figure 26, all sum *L*/*V* ratios on Axles 1 and 3 are less than 1.5 (except for the SEPTA As-is turnout between speeds from 15 to 25 mph in the trailing point runs). In addition to the gage widening, the possibility of wheel climb derailment, as indicated by a greater axle sum *L*/*V* ratio than the threshold value of 1.5 of the Weinstock criterion *(9)* (dry wheel and rail conditions), should not be overlooked for the SEPTA As-is turnout for speeds from 15 to 25 mph in the trailing point runs.

3.4 WEAR INDICES

Wear indices relate the energy dissipated in the wheel/rail contact patch to the wheel wear. In NUCARS™, this is calculated by multiplying the creep forces by the creepages (slips). Separate wear indices are calculated for the tread and flange of each wheel. Units for the wear index are in inch-pounds per inch. The wear index can be seen as a measure of the drag induced in the contact patch, and therefore also relates to the rolling resistance of wheel-on-rail contact.

Figures 27, 28, and 29 give wear indices of left and right wheels of Axle 1 for both the facing point and trailing point runs, respectively, for the SEPTA As-is, AREMA-Case 2, and AREMA As-is turnouts. Barring the huge spikes (about 500,000 pounds-inch per inch of tread wear) in the facing point run at the point of switch in the AREMA As-is turnout, the magnitudes of the energy dissipated in the wheel/rail contact area are more or less of the same order for the SEPTA As-is, AREMA As-is, and the AREMA-Case 2 turnouts. The huge spike occurs because of the kink angle at the point of switch in the AREMA As-is turnout. On average, it would be of negligible consequence on the overall wear in the turnout and should be interpreted as such.

As expected, a two-point contact occurs on the high rail, and a one-point contact occurs on the low rail of the turnouts. This is apparent by finite wear also occurring for the tread of the left wheel in the facing-point diverging-right runs and the tread of the right wheel in the trailing-point diverging-left runs. On the other hand, absences of flange wear on right wheel in the facing point runs and on the left wheel in the trailing point runs indicate a one-point contact. Wear index signatures for both the tread and flange are very uniform (less noise) for the AREMA-Case 2 turnout and nonuniform (more noise) for the SEPTA As-is turnout. A uniformity of wear in the AREMA-Case 2 turnout indicates a smoother ride through this turnout in comparison with the SEPTA As-is turnout.

CHAPTER **4**

FINDINGS AND CONCLUSIONS

The as-built SEPTA tangential design spiraled geometry switch in a Number 8 turnout performs well in comparison with the per-plan AREMA 13-ft curved switch Number 8 turnout. In its intended service, with 5- to 15-mph operations, the switch is superior to the AREMA switch in minimizing loads and accelerations. However, the SEPTA switch does show higher than desired accelerations under B-IV car operations. An improved performance switch can be developed for this particular operation.

Parametric studies of some design features were conducted to determine their effects on switch performance. Tangential switch entry is essential to the good performance of the SEPTA switch. Elimination of a kink angle and its resultant abrupt spike in dynamic loading produce a smooth ride and more even switch wear. The spiral switch entry and exit curves are effective at smoothing the ride through the switch by evening the accelerations. However, the resultant very small radius closure curve may be detrimental for certain types of equipment (i.e., longer cars) or service (higher speeds).

In this particular case, the advantages of the SEPTA switch are not fully utilized with the B-IV cars because of the length of these cars. The extremely short radius closure curves of the switch cause the cars to "stringline," creating relatively high lateral forces. These forces increase rapidly with speed. The AREMA designs, with larger radius closure curves, accommodate the longer cars better at higher speeds.

The use of AMS castings for the switch points in the SEPTA switch produces a tough and durable switch point. When the switches were initially produced, the AMS point was vastly superior to rail steels of the time. However, modern rail steels perform as well as AMS in curve wear. The layout of the switch, with good geometry and guardrails, make the advantages of AMS almost redundant. The high cost of fabricating AMS switch points makes this a costly choice for modern switches.

The housed switch point is a feature that provides benefits for switches with significant diverging traffic. The switch point is thickened to make it more robust and diminish the risk of split switch derailments. The stock rail is diminished to accomplish this, which may result in a foreshortened life for this component. The effect of housing will be to eliminate the sharp dynamic loading and localized wear at the point of switch seen in the field on AREMA switches and in the NUCARS™ simulations done for this study. The running surface discontinuity at the point of switch seen at the gage face is especially important if guardrails are not used in the switch.

Using guardrails in the switch is necessary for safety reasons; the guardrails ensure that a safe operation is maintained as the switch wears and deforms. The guardrail and back of wheel flange contact are nearly vertical, even on worn components. Thus, wheel climb is less likely than with worn wheel flange/switch point contact. As for switch performance, the dynamic loads in the switch are little changed. Switch point life is improved by transferring wear from switch point to guard rail.

Use of guardrails in front of the switch protects the switch points from impacts. The need for, or effectiveness of, the guardrails is diminished by the good switch geometry and housed point design of the SEPTA switch.

The idea of separating the point of switch from the point of curvature (or point of spiral, in the case of the SEPTA switch), where the point of curvature comes first, is good for relatively low speed mainline operations. The mainline trains have to negotiate a small curve as a penalty for making the diverging route curve somewhat larger. This design is a compromise between a lateral switch and an equilateral switch but is biased heavily toward a lateral switch configuration. This also helps the curved switch point at the expense of the straight switch point by lining up wheels for the diverging route curve prior to the switch point, thereby contributing to the good wear performance of the SEPTA switches.

The performance of the replacement option AREMA Number 8 nontangential turnout (designated as AREMA As-is) having an angle at point of 1 deg 41 ft 31 in. is poor to somewhat equivalent as compared with the SEPTA As-is turnout. Very high lateral loads arise due to the entry angle or kink angle of the AREMA As-is turnout. These loads are as high as 20,100 lb at 25 mph on the left wheel of Axle 1 in the facing-point diverging-right run. Even at lower speeds, high lateral loads are produced—as much as 14,300 lb at 5 mph on the left wheel of Axle 1. Performances evaluated in terms of *L/V* ratios, lateral accelerations of axles, bolsters, and car body suggest that AREMA As-is is not on par with the performance of the existing SEPTA As-is turnout.

The performance of the SEPTA As-is switch when used by the B-IV car is highly speed dependent. Up to 15 mph, the SEPTA As-is switch performs better than AREMA type switches of similar lead length. However, performance dimin-

ishes rapidly with operating speeds above 10 to 15 mph. For example, in trailing-point diverging-left runs, lateral loads as much as 21,700 lb at 25 mph are generated on the right wheel of Axle 3. Even though the track curvature layout of this turnout contains a tangential entry to the spiral (840 to 210 ft) with an exit spiral of 210 to 420 ft corresponding to the facing point diverging right runs, the "tightness" of the spiral geometry with respect to the long truck centers and wheelbase of the B-IV cars gives rise to nonsmooth steering through this turnout due to the car body acting as a long rigid chord of the track curve. This chord accommodation to various radii of the track curvature is evidenced by high wheel lateral loads, rapidly changing axle lateral and yaw accelerations, high vertical unloading and loading of the wheels, and high *L*/*V* ratios. A degenerated ride quality is therefore evident for the SEPTA As-is turnout.

Thus, both switch designs have deficiencies for service with the B-IV cars at speeds above 10 to 15 mph. A better switch would employ the good features of each design:

- Tangential switch entry of SEPTA designs and
- Large closure radius of AREMA designs.

The modeled AREMA-Case 2 is an example of this type of switch. The lack of "tightness" of the track curvatures (and consequently the removal of the adverse effects due to car body twist, its chord effect, and rapid changes in axle yaw) are evident in the performance of the B-IV cars on the AREMA-Case 2 turnout. This replacement option consists of a tangential entry to a switch rail of 372-ft radius and a closure rail of the same radius as the switch radius to give a lead length of 59 ft, which is very close to the lead length of the SEPTA As-is turnout.

Smooth steering of B-IV cars through the curvature of the AREMA-Case 2 turnout results for both the facing point and trailing point runs. Wheel lateral loads increase gradually from 5 to 25 mph. This change in the maximum wheel lateral loads from 5 mph to 25 mph is less than 20%. The improved ride quality is also evident from smaller car body lateral and yaw accelerations, reduced axle lateral and yaw accelerations, lesser vertical unloading and loading of the wheels, and lower L/V ratios. The improved ride quality results in tread and flange wear indices that are generally uniform through the turnout curvature, indicating an even wear and probably a longer life for the AREMA-Case 2 turnout.

For speeds less than 15 mph, performance of B-IV cars through the diverging route of the SEPTA As-is turnout is marginal at best. At speeds higher than 15 mph, the ride quality of these "long" cars degrades very fast. Of the various replacement curvatures analyzed, it appears that the AREMA-Case 2 turnout will be the best replacement for the existing SEPTA As-is turnout for all speeds from 5 to 25 mph. The ride quality of the B-IV cars improves significantly through the AREMA-Case 2 turnout curvature as compared with the SEPTA As-is turnout curvature.

The second phase of this project will develop a prototype switch for transit use. The AREMA-Case 2 switch geometry will serve as a starting point for the design of the switch.

REFERENCES

1. Handal, Stephan, “Partial Validation of a Generalized Turnout Model Based on NUCARS™,” *Report R-797*, Association of American Railroads, Washington, D.C. (March 1992).
2. Lord Corporation, V Spring Bonded (for Philadelphia), Drawing Number VSB-1201-10 (February 1990).
3. Wm. Wharton Jr. and Company, Inc., Contract No. 124 for City of Philadelphia, Manganese Switch 840-210 Spiral for Broad Street Subway, Drawing Number V-97163, Easton, Pennsylvania (August 1926).
4. SEPTA, BSS-Erie Avenue Upper Level Special Work, Drawing Number 7-W-16984 (February 1976).
5. AREMA, “Portfolio of Trackwork Plans,” Plan Number 121-62 (1996).
6. FRA, *Track Safety Standards*, Part 213 (1999).
7. Willow, Robert, “Compound Point Geometry,” AREMA Symposium on Turnouts and Special Trackwork (August 1996).
8. Nadal , M. J., “Theorie de la Stabilite des Locomotives,” Part 2, Movement de Lacet, *Annales des Mines*, 10, 232 (1896).
9. Weinstock, H., “Wheel Climb Derailment Criteria for Evaluation of Rail Vehicle Safety,” American Society of Mechanical Engineers Paper 84-WA/RT-1, 1984 ASME Winter Annual Meeting, Phoenix, Arizona (1984).

Abbreviations used without definitions in TRB publications:

AASHO	American Association of State Highway Officials
AASHTO	American Association of State Highway and Transportation Officials
APTA	American Public Transportation Association
ASCE	American Society of Civil Engineers
ASME	American Society of Mechanical Engineers
ASTM	American Society for Testing and Materials
ATA	American Trucking Associations
CTAA	Community Transportation Association of America
CTBSSP	Commercial Truck and Bus Safety Synthesis Program
FAA	Federal Aviation Administration
FHWA	Federal Highway Administration
FMCSA	Federal Motor Carrier Safety Administration
FRA	Federal Railroad Administration
FTA	Federal Transit Administration
IEEE	Institute of Electrical and Electronics Engineers
ITE	Institute of Transportation Engineers
NCHRP	National Cooperative Highway Research Program
NCTRP	National Cooperative Transit Research and Development Program
NHTSA	National Highway Traffic Safety Administration
NTSB	National Transportation Safety Board
SAE	Society of Automotive Engineers
TCRP	Transit Cooperative Research Program
TRB	Transportation Research Board
U.S.DOT	United States Department of Transportation